



### **DISCLAIMER**

This report has been prepared by the Institute of Geological and Nuclear Sciences Limited (GNS Science) exclusively for and under contract to the Earthquake Commission (EQC). Unless otherwise agreed in writing by GNS Science, GNS Science accepts no responsibility for any use of, or reliance on any contents of this Report by any person other than EQC and shall not be liable to any person other than EQC, on any ground, for any loss, damage or expense arising from such use or reliance.

The data presented in this Report are available to GNS Science for other use from July 2009

### **BIBLIOGRAPHIC REFERENCE**

Rhoades, D. A.; Somerville P. G. (Risk Frontiers, Sydney); Dimer de Oliveira, F. (Risk Frontiers, Sydney); Thio, H. K. (URS, Pasadena), 2009. Enhancement of the EEPAS model for long-range earthquake forecasting, *GNS Science Consultancy Report 2009/153*. 47p.

## CONTENTS

<b>EXECUTIVE SUMMARY .....</b>	<b>III</b>
<b>NON-TECHNICAL SUMMARY .....</b>	<b>V</b>
<b>1.0 INTRODUCTION .....</b>	<b>1</b>
<b>2.0 CLASSIFICATION OF EARTHQUAKES BY TECTONIC TYPE .....</b>	<b>2</b>
<b>3.0 MODEL FITTING .....</b>	<b>8</b>
3.1 Overview of models .....	8
3.2 Fitting method .....	10
3.3 Fitting without regard to tectonic type .....	11
3.4 Fitting to earthquakes in separate tectonic classes .....	13
3.4.1 Slab earthquakes .....	13
3.4.2 Interface earthquakes .....	14
3.4.3 Crustal Earthquakes .....	16
3.5 Enhancement of information scores .....	18
<b>4.0 TESTS ON INDEPENDENT DATA .....</b>	<b>19</b>
<b>5.0 CONCLUSION .....</b>	<b>36</b>
<b>6.0 ACKNOWLEDGEMENTS .....</b>	<b>37</b>
<b>7.0 REFERENCES .....</b>	<b>37</b>

## FIGURES

Figure 1	Earthquakes in Japan 1926 – 2005 showing different event types .....	3
Figure 2	Crustal earthquakes in Japan, 1925-2005 .....	4
Figure 3	Interface earthquakes in Japan, 1926 – 2005 .....	5
Figure 4	Slab earthquakes in Japan, 1926 – 2005 .....	6
Figure 5	Cross section of earthquakes through Tohoku, Japan, 1926 – 2005 .....	7
Figure 6	Location of cross section of earthquakes through Tohoku, Japan, 1926 - 2005 .....	8
Figure 7	Predictive scaling relations of long-term seismogenesis derived from examples of the precursory scale increase phenomenon in four well-catalogued regions. (a) Mainshock magnitude $M_m$ versus precursor magnitude $M_p$ ; (b) Precursor time $T_p$ versus $M_p$ ; (c) Precursor area $A_p$ versus $M_p$ . Solid lines are fitted regressions and dotted lines are 95% tolerance limits. After Evison and Rhoades (2004a). .....	9
Figure 8	Map of Japan showing polygonal region of surveillance. ....	11
Figure 9	Normalized rate density (RTR) of earthquake occurrence under the EEPAS model as a function of location (upper), as a function of time (lower left) and as a function of magnitude (lower right). The fixed values are those of the Tottori earthquake of 2000 10 06. The location, time and magnitude of this earthquake are marked on the respective figures. ....	22
Figure 10	Normalized rate density (RTR) of earthquake occurrence under the EEPAS model as a function of location (upper), as a function of time (lower left) and as a function of magnitude (lower right). The fixed values are those of the Niigata-ken-Chuetsu earthquake of 2004 10 06. The location, time and magnitude of this earthquake are marked on the respective figures. ....	23
Figure 11	Normalized rate density (RTR) of earthquake occurrence under the EEPAS model as a function of location (upper), as a function of time (lower left) and as a function of magnitude (lower right). The fixed values are those of the West off Fukuoka earthquake of 2005 03 20. The location, time and magnitude of this earthquake are marked on the respective figures. ....	24
Figure 12	Normalized rate density (RTR) of earthquake occurrence under the EEPAS model as a function of location (upper), as a function of time (lower left) and as a function of magnitude (lower right). The fixed values are those of the Noto-hanto-oki earthquake of 2007 03 25. The location, time and magnitude of this earthquake are marked on the respective figures. ....	25
Figure 13	Normalized rate density (RTR) of earthquake occurrence under the EEPAS model as a function of location (upper), as a function of time (lower left) and as a function of magnitude (lower right). The fixed values are those of the Niigata-ken Chuetsu-oki earthquake of 2007 07 16. The location, time and magnitude of this earthquake are marked on the respective figures. ....	26

Figure 14	Normalized rate density (RTR) of earthquake occurrence under the EEPAS model as a function of location (upper), as a function of time (lower left) and as a function of magnitude (lower right). The fixed values are those of the Iwate-Miyagi earthquake of 2008 06 14. The location, time and magnitude of this earthquake are marked on the respective figures.....	27
Figure 15	EEPAS model forecast of rate density of earthquake occurrence in the slab at hypocentral depth $h \leq 120$ km for magnitude 6.5 on 2009 06 30, based on catalogue up to end of 2005.....	29
Figure 16	EEPAS model forecast of rate density of earthquake occurrence in the slab at depth $h \leq 120$ km for magnitude 7.0 on 2009 06 30, based on catalogue up to end of 2005.....	30
Figure 17	EEPAS model forecast of rate density of earthquake occurrence on the plate interface for magnitude 7.0 on 2009 06 30, based on catalogue up to end of 2005. ....	31
Figure 18	EEPAS model forecast of rate density of earthquake occurrence on the plate interface for magnitude 8.0 on 2009 06 30, based on catalogue up to end of 2005. ....	32
Figure 19	EEPAS model forecast of rate density of earthquake occurrence in the crust for magnitude 6.5 on 2009 06 30, based on catalogue up to end of 2005. ....	33
Figure 20	EEPAS model forecast of rate density of earthquake occurrence in the crust for magnitude 7.0 on 2009 06 30, based on catalogue up to end of 2005. ....	34
Figure 21	Combined EEPAS model forecast of rate density of earthquake occurrence at hypocentral depth $h \leq 120$ km for magnitude 7.0 on 2009 06 30, based on catalogue up to end of 2005.....	35

## TABLES

Table 1	Parameters and information scores for EEPAS model fitted to Japan catalogue, without regard to tectonic type.....	12
Table 2	Parameters and information scores for EEPAS model fitted to slab earthquakes in the Japan catalogue ( $N = 42$ ). EEPAS parameters not listed are constrained to the same values as in Table 1.....	14
Table 3	Parameters and information scores for EEPAS model fitted to interface earthquakes in the Japan catalogue ( $N = 21$ ). EEPAS parameters not listed are constrained to the same values as in Table 1. ....	15
Table 4	Parameters and information scores for EEPAS model fitted to interface earthquakes in the Japan catalogue ( $N = 42$ ). The PPE model is derived using interface and shallow slab earthquakes. The time-varying component of EEPAS is derived from interface earthquakes only. ....	15
Table 5	Parameters and information scores for EEPAS model fitted to crustal earthquakes in the Japan catalogue ( $N = 42$ ). EEPAS parameters not listed are constrained to the same values as in Table 1. ....	17
Table 6	Parameters and information scores for EEPAS model fitted to crustal earthquakes in the Japan catalogue ( $N = 42$ ). The PPE model is derived using crustal and interface earthquakes. The time-varying component of EEPAS is derived from crustal earthquakes only. ....	18
Table 7	Information scores for best model in each class and best combined model in fitting to the learning set (1966-1995).....	19
Table 8	Information scores for best model in each class and best combined model evaluated on the testing set of earthquakes (1996-2005).....	20
Table 9	Earthquakes ( $M > 5.95$ ) in the region of surveillance during the test period, 1996-2005, and normalised rate densities under the SUP, PPE and EEPAS models taking tectonic type into account. ....	28

## APPENDICES

Appendix 1	Technical Description of SUP Model.....	39
Appendix 2	Technical description of PPE Model .....	39
Appendix 3	Technical Description of EEPAS Model .....	40

## EXECUTIVE SUMMARY

The EEPAS model, which regards Every Earthquake as a Precursor, According to Scale, of larger earthquakes to follow it in the long-term, is showing promise as a long-range earthquake forecasting method, which is demonstrably informative in several seismically active regions, including New Zealand, California and Japan. In previous applications of the model all earthquakes have been treated uniformly, regardless of their tectonic setting: those occurring within the continental crust; those on plate boundaries; and those within subducted slabs. However, earthquakes within a given tectonic category are expected to have a stronger correlation than earthquakes from different tectonic categories.

The objective of this work is to enhance the application of the EEPAS model by distinguishing the three tectonic categories of earthquake. Using the SEIS-PC earthquake catalogue of Japan for magnitude  $M \geq 4$ , the tectonic type of each earthquake was assigned using a definition of the plate boundaries by Gudmundsson and Sambridge. The period from 1966-1995 was used as a learning set for fitting models, and 1996-2005 as a testing set for confirmation of the results, with the target earthquakes being those with magnitude  $M \geq 6$ . There are 105 target earthquakes in the learning set (42 slab, 21 interface and 42 crustal) and 37 in the testing set (13 slab, 7 interface and 17 crustal).

The inspiration for the EEPAS model comes from the “precursory scale increase” phenomenon – an increase in the rate and magnitude of minor earthquakes, which precedes most major earthquakes in the long term – and its associated predictive scaling relations. The model is a mixture of a time-varying component based on this phenomenon, and the Proximity to Past earthquakes (PPE) model – a kind of smoothed seismicity model. The latter model also serves as a useful reference model which is spatially varying but in principle time-invariant.

Models were fitted using the maximum likelihood method. The goodness of fit of a model is measured by an information score which takes into account the log likelihood of the data under the model and the number of fitted parameters, and is normalized by the number of targeted earthquakes.

Fitting of the EEPAS and PPE models to the learning set, targeting the earthquakes of particular tectonic types, has shown that:

1. Large earthquakes in the slab tend to occur near to where large earthquakes have previously occurred either in the slab or on the plate interface, and that the earthquakes precursory to large earthquakes in the slab may occur either in the slab or on the interface, but hardly ever in the crust.
2. Large interface earthquakes tend to occur where large earthquakes have previously occurred either on the interface or in the shallow part of the slab. Also, the precursory earthquakes for interface events nearly all occur on the interface itself.
3. Large earthquakes in the crust tend to occur near to where large earthquakes have previously occurred either in the crust or on the plate interface. Also, the precursory earthquakes for crustal events mainly occur in the crust.

Taking tectonic type into account, the optimal EEPAS model uses slab and interface events as precursors to major slab earthquakes, interface events only as precursors to major interface events, and crustal events only as precursors to major crustal events. For the smoothed-seismicity component of the EEPAS model, it is optimal to use slab and interface events to forecast the location of earthquakes in the slab, interface events only to forecast the location of earthquakes on the interface, and both crustal and interface events to forecast the location of events on the interface. The combined optimal models fit the learning data set data much better than an EEPAS model which does not take account of tectonic type, with the information score being increased by 0.38. This corresponds to an average probability gain per earthquake of about 1.5. The information score is higher for earthquakes in the slab and on the interface than for crustal earthquakes.

When the optimal models were applied to the independent testing period, a similar overall information gain was obtained compared with a model which does not take account of tectonic type. A difference was that the information gain of the EEPAS model over the PPE model was higher for crustal earthquakes, and lower for slab and interface earthquakes, than in the learning period.

Distinguishing the three tectonic categories of earthquake has thus generally confirmed the hypothesis that earthquakes interactions are stronger between earthquakes of similar tectonic types than between those of different types, and has resulted in an improved forecasting model for the Japan region.

A detailed analysis of six individual major crustal earthquakes in the testing period showed that the new EEPAS forecast was quite informative for occurrence of the Tottori (2000) and Niigata-ken Chuetsu (2004) earthquakes, uninformative for the West off Fukuoka (2005) and Noho-hanto-oki (2007) earthquakes, and somewhat informative for the Niigata-ken Chuetsu-oki (2007) and Iwate-Miyagi (2008) earthquakes.

The Japan catalogue was used for this research because a plate interface model was available to readily separate it into tectonic categories and because the long instrumental record and high rate of earthquake occurrence facilitate statistical testing of the method. The results are highly relevant to New Zealand conditions because Japan has a similar tectonic environment, including subduction zones and large strike-slip faults. Therefore, it is likely that a similar improvement in forecasting performance could be obtained by applying these methods to the New Zealand catalogue.

## NON-TECHNICAL SUMMARY

The EEPAS model is a long-range earthquake forecasting method, which is showing promise in forecasting major earthquakes in several regions, including New Zealand, California and Japan. This model uses all the previous earthquakes in the catalogue to forecast the probability of future earthquakes occurring at future times, magnitudes and locations. It relies on a precursory increase in the rate and magnitude of minor earthquakes, which precedes most major earthquakes in the long term.

In some regions located on the boundary between two tectonic plates, including New Zealand and Japan, the edge of one tectonic plate is forced under the edge of another. Then it is possible to distinguish three types of earthquake: *slab* earthquakes occurring within the lower plate, *interface* earthquakes occurring close to the plate boundary, and *crustal* earthquakes occurring within the upper plate. The objective of this study is to improve the EEPAS model by distinguishing these three types of earthquake.

The earthquake catalogue of Japan with magnitude  $M \geq 4$  was used and each earthquake was classified as slab, interface or crustal. The period from 1966-1995 was used as a learning period for fitting models, and 1996-2005 as a testing period for confirmation of the results, with the target earthquakes being those with magnitude  $M \geq 6$ . There are 105 target earthquakes in the learning set (42 slab, 21 interface and 42 crustal) and 37 in the testing set (13 slab, 7 interface and 17 crustal).

Fitting of the EEPAS model to the learning period has shown that:

- 1 Major slab earthquakes tend to occur near to where major slab or interface earthquakes have occurred previously, and minor slab and interface earthquakes tend to occur as precursors to major slab earthquakes.
- 2 Major interface earthquakes tend to occur where major interface or shallow slab earthquakes have occurred previously, and minor interface earthquakes tend to occur as precursors to major interface earthquakes.
- 3 Major crustal earthquakes tend to occur near to where major crustal or interface earthquakes have occurred previously, and minor crustal earthquakes tend to occur as precursors to major crustal earthquakes.

The fit of the EEPAS model to the learning set is improved by using only slab and interface events to forecast major slab earthquakes, only interface events to forecast major interface events, and only crustal events to forecast major crustal events. This new model fits the slab and interface earthquakes better than it does the crustal earthquakes. The improvement in forecasting performance was confirmed by applying the new model to the testing period.

The Japan catalogue was used because it is large and the earthquake types are relatively easy to assign. The results are relevant to other similar regions, such as New Zealand. Therefore, an improvement in forecasting performance could probably be obtained by applying the same methods to the New Zealand catalogue.

## 1.0 INTRODUCTION

The EEPAS model, which regards Every Earthquake as a Precursor, According to Scale, of larger earthquakes to follow it in the long-term, is showing promise as a long-range earthquake forecasting method. It was originally fitted to the New Zealand earthquake catalogue to optimise its performance in forecasting earthquakes of magnitude  $M > 5.75$ . With unchanged parameters, it has been shown to outperform a spatially varying Poisson model based on proximity to the locations of past earthquakes (PPE) in California for magnitude  $M > 5.75$  (Rhoades and Evison, 2004) and in Japan for  $M > 6.75$  (Rhoades and Evison, 2005). It has also been applied at lower magnitudes ( $M > 4.75$  and  $M > 4.95$ , respectively) to high-quality catalogues of the Kanto region, central Japan, and southern California (Rhoades and Evison, 2006; Rhoades, 2007), and at  $M > 5.95$  in Greece (Console et al. 2006) and  $M > 4.25$  in south-eastern Australia (Somerville et al., 2006), all with similarly successful results.

The use of a time-dependent earthquake forecast like EEPAS can potentially provide much improved estimates of earthquake hazard in a given region during a given year. Damaging earthquakes are likely to occur in some but not all locations that are identified as having an increased level of activity. For a particular location and magnitude, the rate density can vary over time by as much as a factor of 5 or 10 times higher or lower than the long-run average level. This proposal is aimed at further improvement of the model which already has demonstrated skill in forecasting earthquakes on a time-scale of a few years.

As presently formulated, the EEPAS model is in a certain sense rather crude, in that it treats all earthquakes the same, regardless of their tectonic setting. For example, it does not discriminate between three distinct tectonic categories of earthquakes: those occurring within the continental crust; those on plate boundaries; and those within subducted slabs. In regions such as Japan and New Zealand, earthquakes in two or more of these categories occur in close horizontal (but not necessarily vertical) proximity, because of the subduction processes that are such an important feature of the seismotectonics of these regions. As presently implemented in EEPAS, this proximity causes earthquakes from different tectonic categories to interact with each other in the forecast process. However, earthquakes within a given tectonic category are expected to have a stronger correlation than earthquakes from different tectonic categories.

Notwithstanding this expectation, it should be noted that there is anecdotal evidence of apparent short-term interactions between large earthquakes across earthquake categories. Examples include the 1942 Wairarapa earthquakes, in which a large earthquake in the crust was followed by one in the slab within a few months (Doser and Webb, 2003); and the 1990 Weber earthquakes, in which a large earthquake in the slab was followed by one on the plate interface within a few months (Anderson, 1991). There may also be longer term interactions. It has been suggested by Shimazaki (1976) that large interplate earthquakes on subduction zones along the Pacific coast in Japan are preceded (over a period of decades) by an increase in the level of activity of large intraplate earthquakes within the crust of the overriding plates, due to the high intraplate stress caused by the loading of the plate interface.

How the long-term seismogenic process is affected by tectonic setting should be revealed by different optimal EEPAS parameters for earthquakes in different tectonic categories and

different interactions between earthquakes within a given tectonic category than between earthquakes in different categories. Therefore, in this study we examine the hypothesis that the long-term seismogenic process for a major earthquake is affected by its tectonic setting, and that the EEPAS model can be improved by taking account of the tectonic category to which precursory earthquakes belong.

The objective of this work is to enhance the application of the EEPAS model by distinguishing these three categories of earthquake. Accordingly, we elaborate the EEPAS model by separating earthquakes into the three tectonic categories and developing the EEPAS parameters for each one. We fit the EEPAS model independently to each earthquake category, and then combine the models and measure the improvement in forecast performance that is obtained.

## 2.0 CLASSIFICATION OF EARTHQUAKES BY TECTONIC TYPE

The main catalogue of Japan used in this study is that provided by the SEIS-PC earthquake analysis package developed by Y. Ishikawa. In previous studies of EEPAS in Japan, the catalogue produced by the Japan Meteorological Agency (JMA) has been used, but the JMA catalogue has recently undergone a major revision and the revised catalogue and its updates are no longer freely available to researchers outside of certain agencies and research organisations in Japan. The SEIS-PC catalogue appears to be of similar quality to the JMA catalogue and has the advantage that it is freely available. Within the area of study adopted here (Figure 1) it appears to be more complete than the JMA catalogue.

The definition of the plate boundaries by Gudmundsson and Sambridge (1998) was used to define the plate interfaces in Japan. We calibrated this against the locations of events having known accurate depths and earthquake categories. We also calibrated it against the larger set of events based on the International Seismological Centre (ISC) catalogue having accurate focal depths (Engdahl, et al, 1998). Since that catalogue has poor completeness, we then calibrated the SEIS-PC catalogue against the ISC catalogue. The end result is a complete catalogue that has event type assigned.

The whole earthquake catalogue is displayed in map view in Figure 1, which shows the three different earthquake categories. Maps of the individual earthquake categories are shown in Figures 2, 3 and 4, which show depth by colour coding. A cross section across Tohoku is shown in Figure 5, and the location of the cross section is shown in Figure 6.

For the large majority of the events, i.e., the smaller ones, this assignment is "statistical" in the sense that it is based on the estimate of focal depth alone, without knowing the actual event type. This is the best that can be done because the event types of the smaller events are not known.

The assignment is based on the distance of the hypocenter from the plane defining the plate boundary. Events within, say, 5 km of the plate boundary are assumed to be interface events. Events more than 5 km above it are assumed to be crustal events. Events more than 5 km below it are assumed to be slab events. The threshold values are arbitrary, and one could in principle experiment with different values. It is recognised that some earthquakes are inevitably misclassified. However, the tectonic types are regarded as fixed for the purposes of the analyses carried out here. This is reasonable, because the seismicity models fitted here are also "statistical", and do not depend upon a perfect classification.

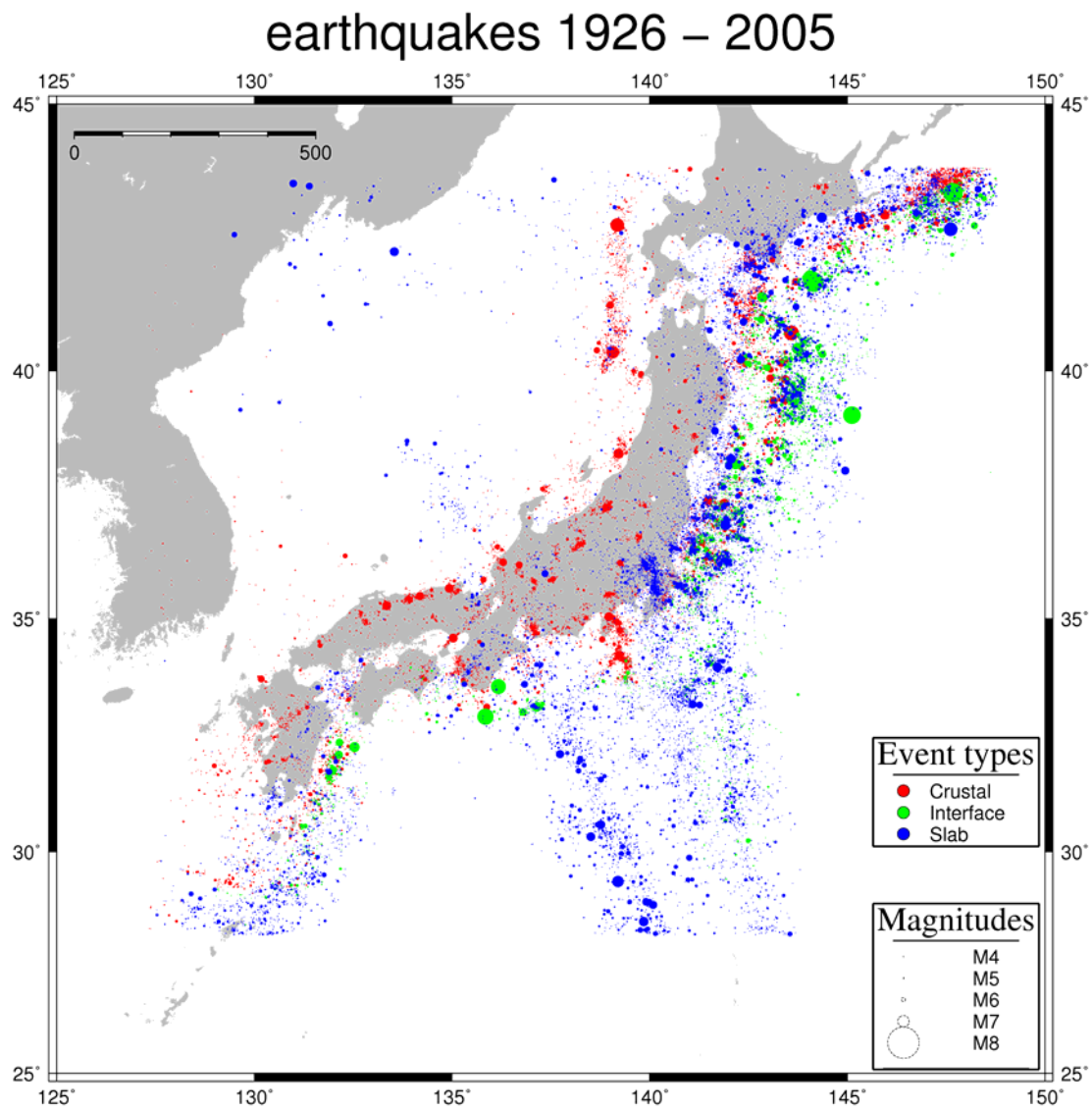


Figure 1 Earthquakes in Japan 1926 – 2005 showing different event types

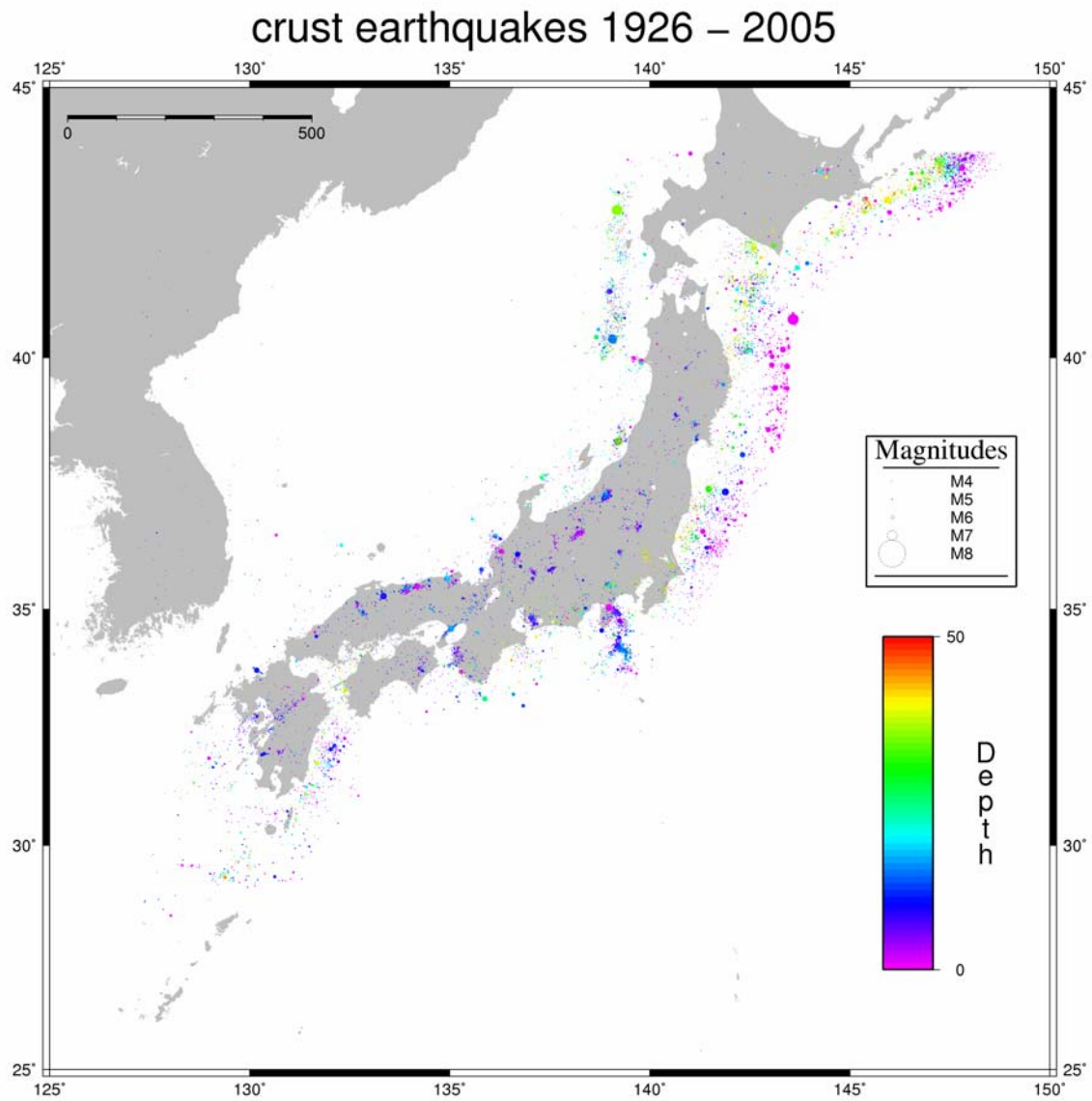


Figure 2 Crustal earthquakes in Japan, 1925-2005

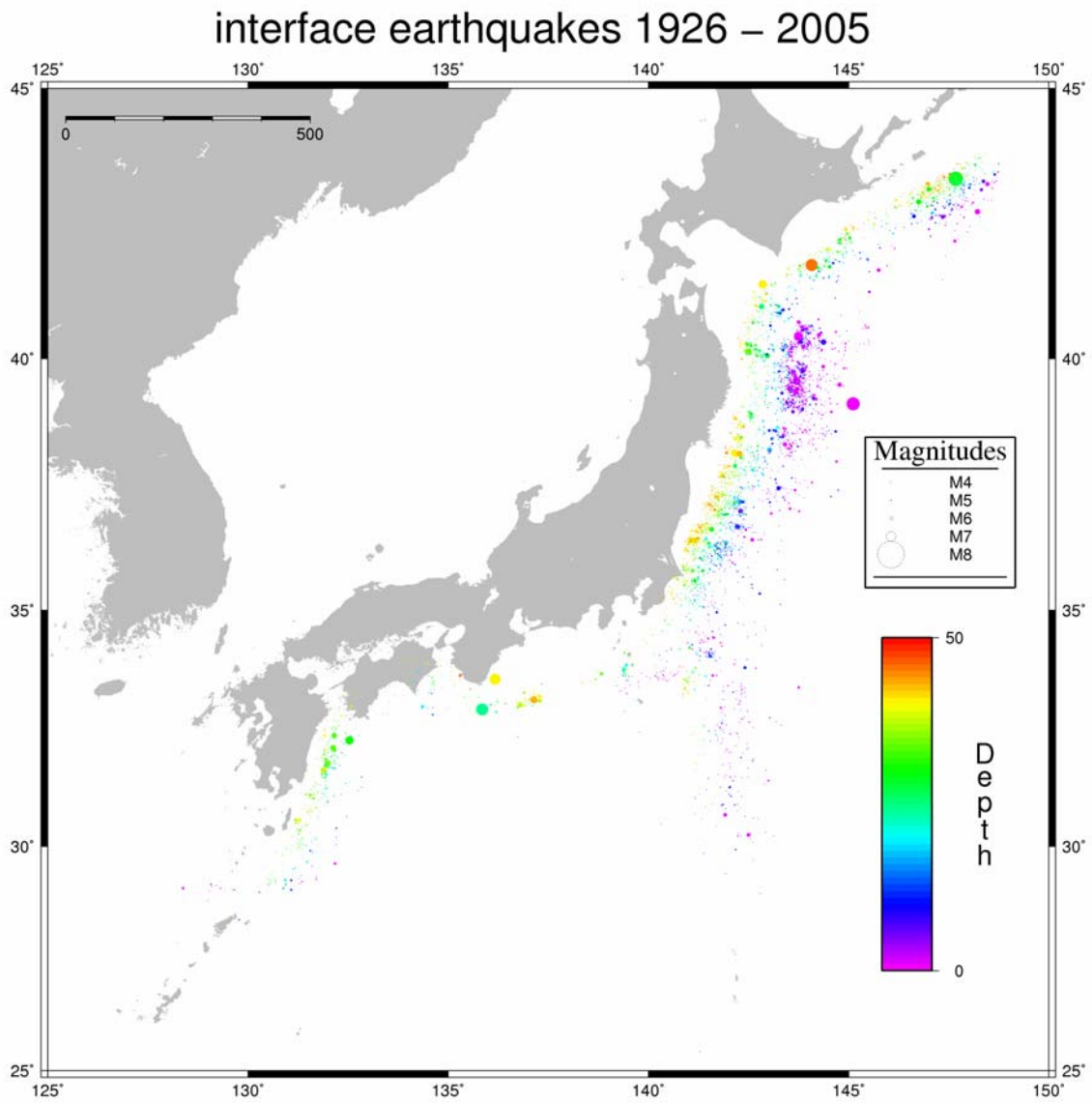


Figure 3 Interface earthquakes in Japan, 1926 – 2005

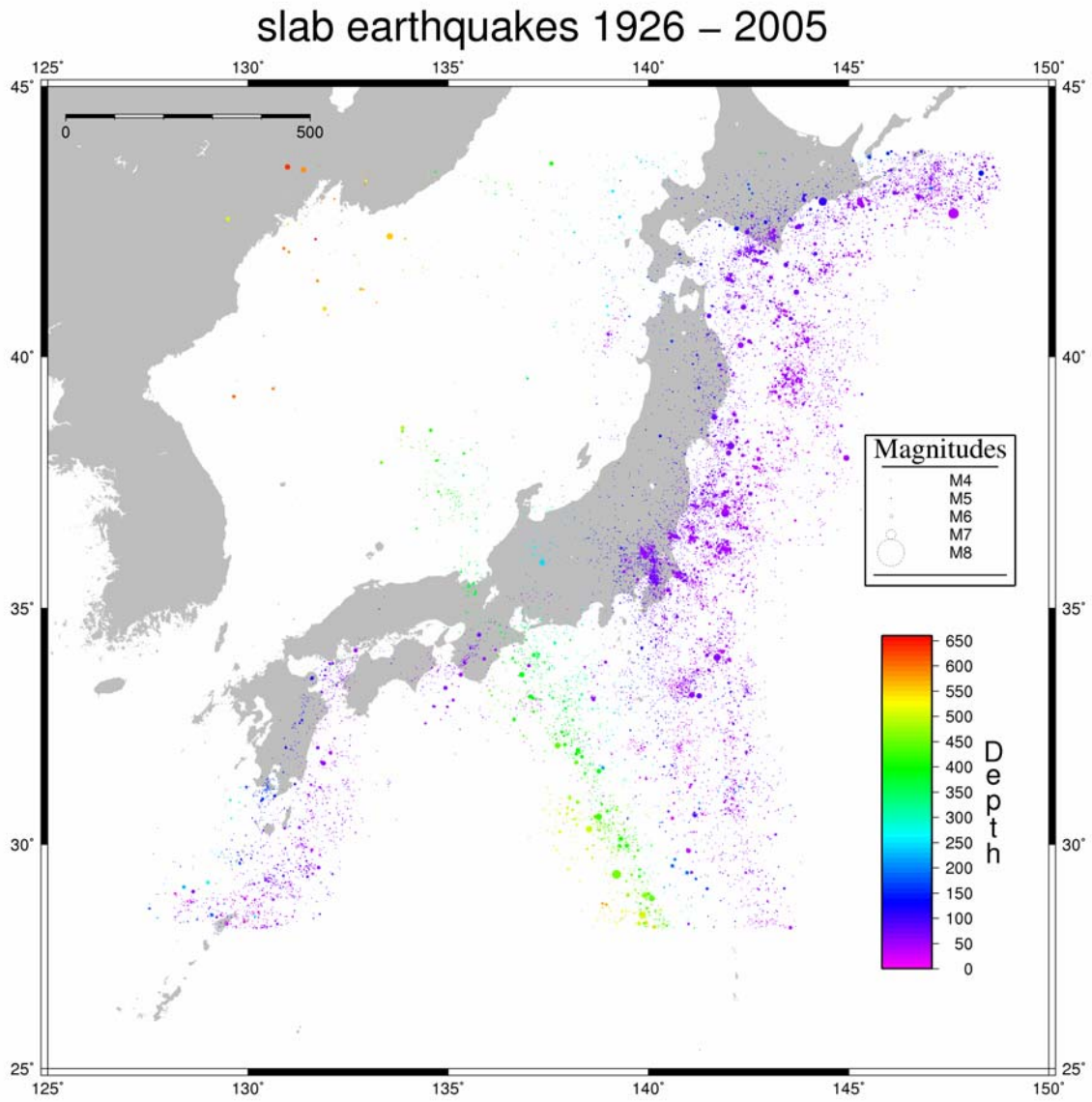


Figure 4 Slab earthquakes in Japan, 1926 – 2005

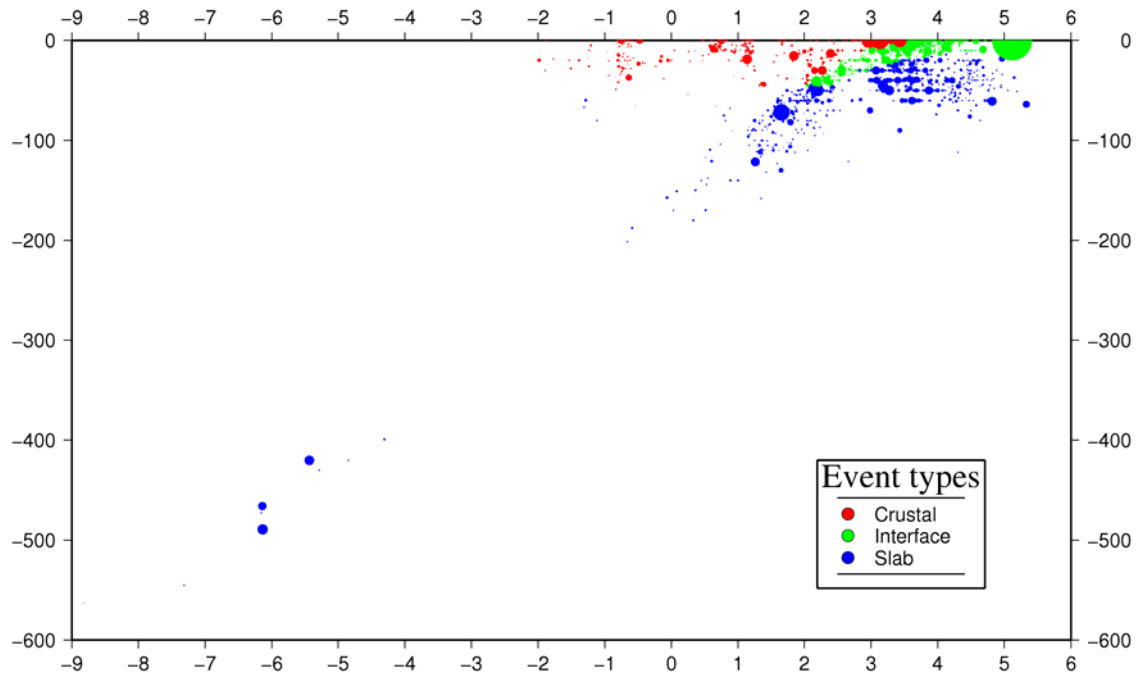


Figure 5 Cross section of earthquakes through Tohoku, Japan, 1926 – 2005

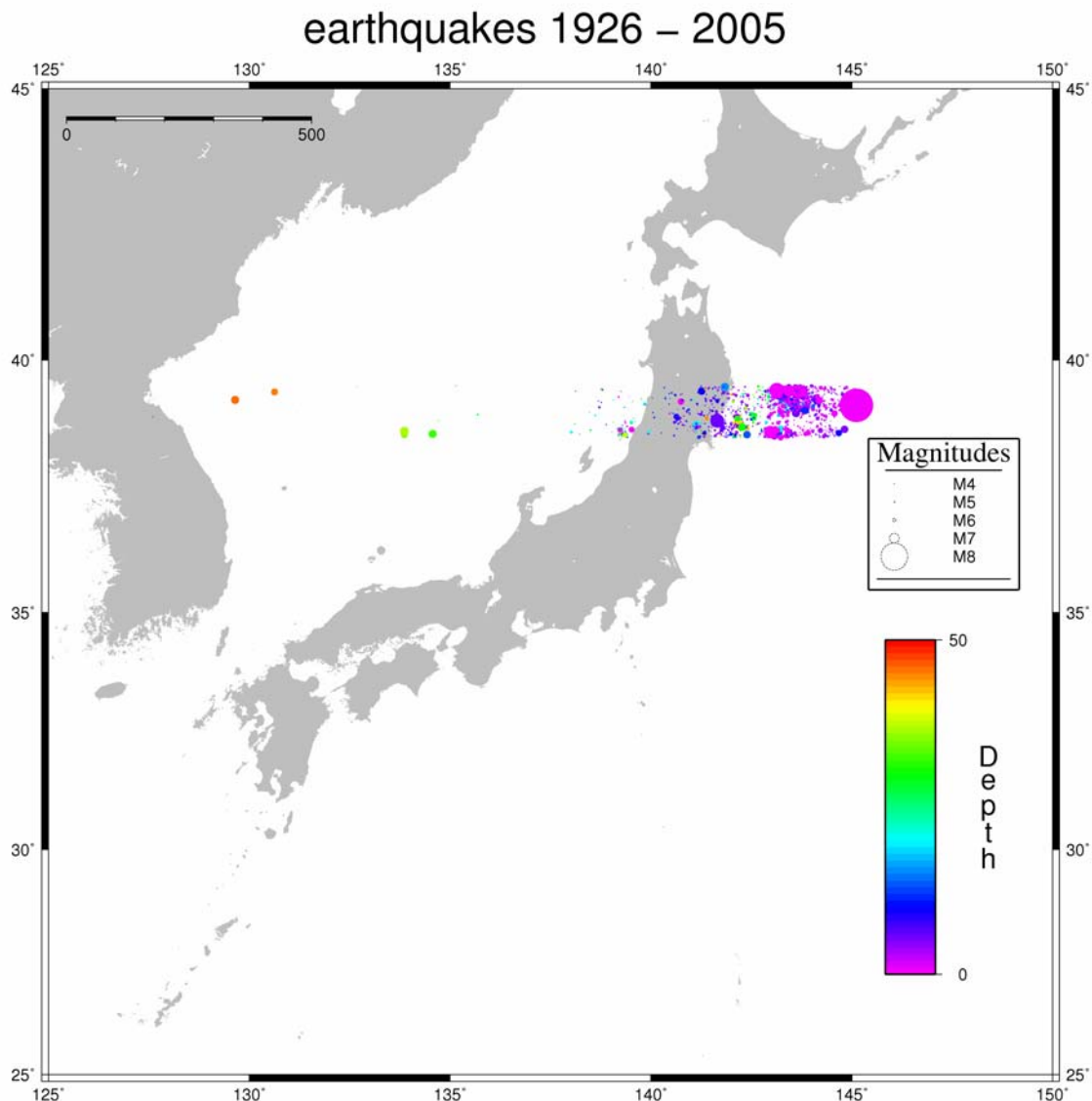


Figure 6 Location of cross section of earthquakes through Tohoku, Japan, 1926 - 2005

### 3.0 MODEL FITTING

#### 3.1 Overview of models

The EEPAS model is based on an increase in the rate and magnitude of minor earthquakes, which has been found to precede most major earthquakes in the long term in several well-catalogued regions of the world. This increase is known as the “precursory scale increase” (Evison and Rhoades, 2001, 2002, 2004a,b, 2005; Papadimitriou et al., 2006). A special case of the precursory scale increase is the precursory swarm phenomenon (Evison, 1977, 1982; Evison and Rhoades, 1993, 1997, 1999, 2000). Associated with the precursory scale increase are the predictive scaling relations – regressions of mainshock-magnitude, precursor-time, and precursory area on the precursory magnitude level (Figure 7). These relations allow the magnitude, time of occurrence and source area of a major earthquake to be predicted from the precursory magnitude level. The EEPAS model treats each earthquake

as a possible long-term precursor, and uses the predictive scaling relations, together with the earthquake's magnitude, to estimate the distribution in time, magnitude and location, of the earthquake's contribution to the future earthquake occurrence rate density.

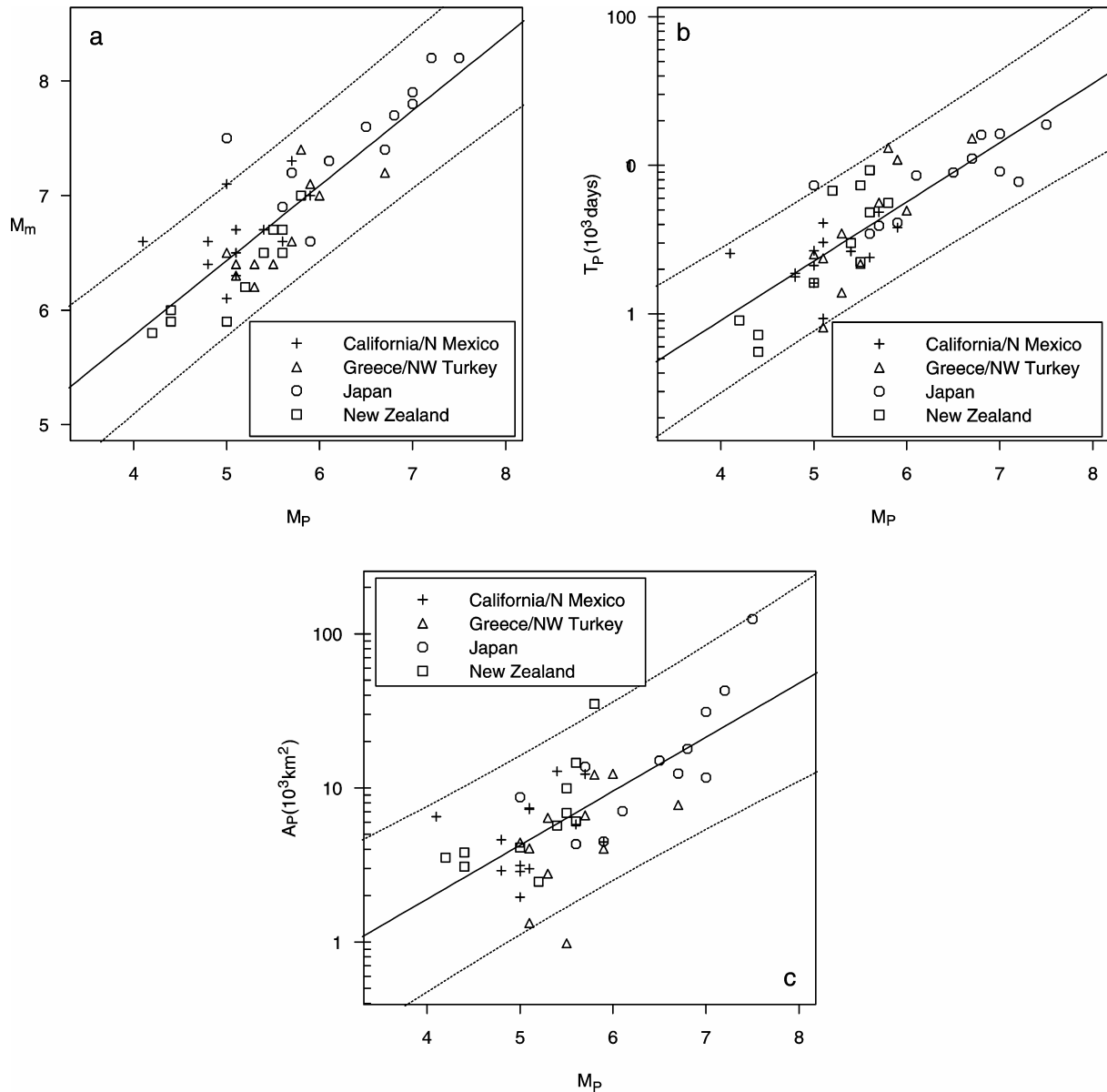


Figure 7 Predictive scaling relations of long-term seismogenesis derived from examples of the precursory scale increase phenomenon in four well-catalogued regions. (a) Mainshock magnitude  $M_m$  versus precursor magnitude  $M_p$ ; (b) Precursor time  $T_p$  versus  $M_p$ ; (c) Precursor area  $A_p$  versus  $M_p$ . Solid lines are fitted regressions and dotted lines are 95% tolerance limits. After Evison and Rhoades (2004a).

The parameters of the EEPAS model are closely linked to the predictive scaling relations:  $a_M$ ,  $b_M$  and  $\sigma_M$  to the intercept, slope and standard deviation, respectively, of the regression of mainshock magnitude on precursor magnitude;  $a_T$ ,  $b_T$  and  $\sigma_T$  to the intercept, slope and standard deviation, respectively, of the regression of the logarithm of precursor time on

precursor magnitude; and  $b_A$  and  $\sigma_A$  to the slope and intercept, respectively, of the regression of the logarithm of precursor area on precursor magnitude.

The EEPAS model is a mixture of a time-varying component based on the precursory scale increase phenomenon, as described above, and the Proximity to Past earthquakes (PPE) model – a kind of smoothed seismicity model. The PPE model is based on the notion that large earthquakes occur close to where they have occurred in the past.

Another model that plays an important underlying role in the analyses presented here is the Stationary Uniform Poisson (SUP) model. In this model, the magnitude distribution conforms to the Gutenberg-Richter frequency magnitude relation, but the rate of earthquake occurrence is both temporally and spatially invariant. The SUP model is useful as a model of “least information”, and as such it is the baseline for information scores defined in the next section. By comparison, the PPE model also conforms to the Gutenberg-Richter relation and the rate of earthquake occurrence is in principle time-invariant (although continually updated as new earthquakes occur) but spatially varying. On the other hand, in the EEPAS model, the rate of earthquake occurrence is essentially both temporally and spatially varying, and in small space time volumes does not conform to the Gutenberg-Richter relation.

Technical details of the SUP, PPE and EEPAS models are given in the Appendix.

### 3.2 Fitting method

Fitting is carried out by maximum likelihood, and quantification of improvements is carried out using the likelihood method, which is widely recognised as an appropriate method for comparison of probabilistic forecasting models, and is the method adopted by the earthquake forecast testing centres (Rhoades and Evison, 1989; Jackson, 1996; Schorlemmer and Gerstenberger, 2007; Schorlemmer et al. 2007).

The outcome of the research is a model which is an elaboration of the standard EEPAS model for Japan. A more elaborate model is bound to fit the data better (i.e. have a higher likelihood) than the original model. The assessment of statistical significance of the improvement is rigorously achieved by splitting the catalogue into two sets – a learning set and a testing set. The model fitting is carried out on the learning set, and the formal performance assessment and significance testing on the testing set. In order to avoid the well-known problems associated with over-fitting, a goodness of fit statistic which includes a penalty for fitting extra free parameters is used. At the testing stage, the number of fitted parameters is irrelevant because there are no free parameters. By comparing goodness of fit or performance statistics of the PPE and SUP models, we can measure the information value of spatial variation of earthquake occurrence under the PPE model. And by comparing similar statistics of the EEPAS and PPE models, we can measure the information value of time-variation of earthquake occurrence under the EEPAS model. If over-fitting is successfully avoided, the information value of models tends to be similar whether assessed at the fitting stage or the testing stage.

The goodness of fit is assessed using the Akaike Information Criterion (AIC) statistic (Akaike, 1974), defined for a particular model  $M$  as

$$AIC_M = -2 \ln L_M + 2p_M \quad , \quad (1)$$

where  $\ln L_M$  is the optimised log likelihood of the model, and  $p_M$  is the number of fitted parameters. A relatively low value of AIC indicates a relatively high information value, a model which explains the data relatively well. Formally the information value of a fitted model is expressed as the information rate per earthquake,  $I_M$ , defined by

$$I_M = (AIC_{SUP} - AIC_M) / (2N) \quad (2)$$

where  $N$  is the number of earthquakes in the target set.

The fitting period is 1965 January 1 to 1995 December 31. Only earthquakes with hypocentral depth  $h \leq 120$  km are used. The targeted earthquakes are those inside the polygonal region of surveillance shown in Figure 8. The region of surveillance was chosen to be as large as possible, in order to obtain the maximum possible number of earthquakes in each tectonic subset, subject to adequate catalogue completeness for precursory earthquakes. The magnitude threshold  $m_0$  for earthquakes contributing to the analysis is 3.95 and the magnitude threshold  $m_c$  for targeted earthquakes is 5.95.

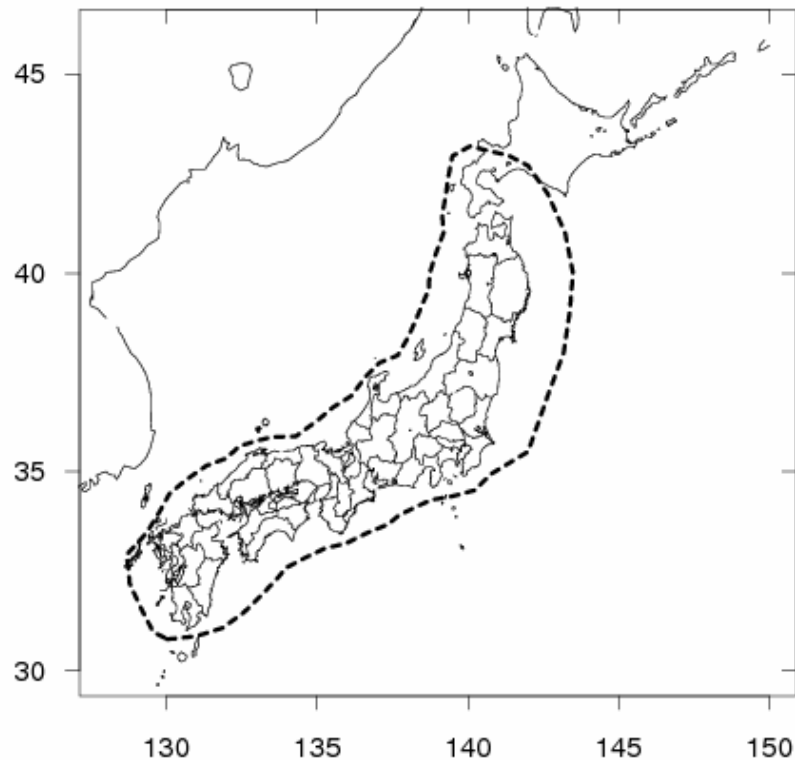


Figure 8 Map of Japan showing polygonal region of surveillance.

### 3.3 Fitting without regard to tectonic type

First the SUP, PPE and EEPAS models were fitted to earthquakes in the Japan catalogue without regard to tectonic type. Note that all earthquakes with  $h > 45$  km are classified as in the slab. We also examine the fit in the case that only earthquakes with  $h \leq 45$  km are used.

The information rate is not usually improved greatly by fitting many parameters. Here we fit only four parameters of the EEPAS model ( $a_M$ ,  $a_T$ ,  $\sigma_A$  and  $\mu$ ), with other parameters being fixed at typical values from previous studies. The equal-weights version of the EEPAS model (Rhoades and Evison, 2004) is used. Here, and in all fits to subsets below, the “failure-rate” parameter  $\mu$  is constrained to lie in the range from 0 to 0.5. The optimal value of 0.5 (Table 1) indicates that the EEPAS model is a 50:50 mixture of the time-varying component of EEPAS and the static component (the PPE model). This is a high value of  $\mu$  compared to the values estimated in previous studies (Rhoades and Evison, 2004, 2005, 2006), which are typically much nearer to 0.

It can be seen from Table 1 that the fitted parameter values are very similar for the two cases of  $h \leq 120$  km and  $h \leq 45$  km. Also the information rates are similar, indicating that the EEPAS model forecasts the deeper earthquakes in the range  $45 < h \leq 120$  km just as well as the shallower earthquakes with  $h \leq 45$  km.

The difference  $\Delta I$  between  $I_{EEPAS}$  and  $I_{PPE}$  is an indicator of the amount of time-varying information provided by the EEPAS model. From Table 1 the difference is 0.16 for  $h \leq 120$  km and 0.13 for  $h \leq 45$  km. These values correspond to an average probability gain per earthquake of 1.15 and 1.19, respectively. The observed values of  $\Delta I$  are similar to the value of 0.13 obtained by Rhoades and Evison (2005) in fitting the same models (but with  $\mu = 0$ ) to a larger region of surveillance using the Japan Meteorological Agency (JMA) catalogue with  $m_c = 6.25$ . They are however much lower than values of  $\Delta I$  obtained from studies of the EEPAS model in California, which range from 0.72 (Rhoades and Evison, 2004) for the whole of California with  $m_c = 5.75$  to 0.82 (Rhoades, 2007) for Southern California with  $m_c = 4.95$ . The high information value of the EEPAS model in California has been ascribed to the fact that the plate boundary tectonics in California is relatively simple and most of the seismicity is shallower than 15 km (Rhoades and Evison, 2006).

Table 1 Parameters and information scores for EEPAS model fitted to Japan catalogue, without regard to tectonic type.

Parameter	Depth restriction	
	$h \leq 120$ km ( $N=105$ )	$h \leq 45$ km ( $N=76$ )
	<b>Fixed or fitted values</b>	
$a_M$	1.47	1.48
$b_M$	1.0*	1.0*
$\sigma_M$	0.32*	0.32*
$a_T$	1.43	1.42
$b_T$	0.4*	0.4*
$\sigma_T$	0.23	0.23*
$b_A$	0.35*	0.35*
$\sigma_A$	1.06	1.07
$\mu$	0.50	0.50
<b>Information score</b>	<b>Value</b>	
$I_{PPE}$	1.42	1.44
$I_{EEPAS}$	1.58	1.57
$\Delta I = I_{EEPAS} - I_{PPE}$	0.16	0.13

\* Fixed parameter value

### 3.4 Fitting to earthquakes in separate tectonic classes

Next we fit the models with the target set of earthquakes restricted to individual tectonic-type subsets. We consider different predictor sets, in order to determine whether the precursors of major earthquakes in a particular tectonic class come from the same class or different classes of earthquakes. The polygon and time-period for the target earthquakes are the same as in the previous section.

#### 3.4.1 Slab earthquakes

There are 42 slab earthquakes in the target set, including 29 with  $h \geq 45$  km. Although the predictability of the shallower slab events with  $h \leq 45$  km is of some interest in its own right, there are only 13 events from this class in the target set. This subset is not considered large enough for dependable fitting as a separate class. Therefore we consider only the predictability of all the slab events together as a single class.

Table 2 shows the result of fitting the models to these data for different predictor sets of earthquakes (slab, crust and slab, interface and slab, and all earthquakes). Note that the largest values of  $I_{EEPAS}$ ,  $I_{PPE}$  and  $\Delta I$  are all attained when both interface and slab events are included in the predictor set. Since the PPE model embodies the hypothesis that large earthquakes tend to occur near to where they have occurred before, the result for  $I_{PPE}$  suggests that large earthquakes in the slab tend to occur near to where large earthquakes have previously occurred either in the slab or on the interface. The results for  $I_{EEPAS}$  and  $\Delta I$  together imply that the earthquakes precursory to large earthquakes in the slab may occur either in the slab or on the interface, but hardly ever in the crust. This analysis does not show whether or not it is only relatively shallow slab earthquakes close to the interface which have precursors on the interface.

Note that the values of  $I_{EEPAS}$ ,  $I_{PPE}$  and  $\Delta I$  in Table 2 are all much higher than those in Table 1. It follows that earthquakes in the slab are on average much more predictable than earthquakes in general in the target region, using any of the predictor sets in Table 2. The optimum value of 0.59 for  $\Delta I$  indicates that the amount of time-varying information for slab earthquakes is very much greater than that for earthquakes in general in Table 1, and not much less than that found in the studies of California.

Comparing the fitted parameter values for the optimal model in Table 2 with those in Table 1, we note that the values of  $a_M$  and  $\sigma_A$  are rather similar. The value of  $a_T$  (1.15) for slab earthquakes is less than that in Table 1 (1.43). If all other parameter values were equal, this difference would indicate that earthquakes in the slab have a precursor time which is shorter on average by a factor of 0.52 than earthquakes in general in the target region. Also we note that the parameter  $\mu$  of the optimal model, at 0.34, is less than that in Table 1. A lower value of  $\mu$  indicates that a higher proportion of the target earthquakes have precursory sequences conforming well to the fitted EEPAS model parameters. Again, this analysis does not show whether or not it is the relatively shallow slab earthquakes close to the interface which conform best to the EEPAS model parameters of the optimal model.

It is instructive also to compare the parameter values obtained with slab earthquakes only in the predictor set with those of the optimal model when slab and interface events are both included. The high value of 1.7 for the parameter  $a_M$  indicates that the precursory earthquakes occurring in the slab have relatively low magnitudes. Because of this high value

of  $a_M$ , the relatively large values of  $a_T$  and  $\sigma_A$  should not be taken to indicate relatively long precursor times and large precursor areas, respectively. The relatively high value of 0.49 for  $\mu$  indicates that a relatively high proportion of target earthquakes do not have precursory sequences in the slab conforming to the fitted EEPAS parameters.

Table 2 Parameters and information scores for EEPAS model fitted to slab earthquakes in the Japan catalogue ( $N = 42$ ). EEPAS parameters not listed are constrained to the same values as in Table 1.

	<b>Predictor set</b>			
	Slab	Crust +slab	Interface +slab	Crust +interface +slab
<b>Parameter</b>	<b>Fitted values</b>			
$a_M$	1.70	1.70	1.52	1.45
$a_T$	1.31	1.25	1.15	1.09
$\sigma_A$	1.10	0.60	0.96	0.94
$\mu$	0.49	0.50	0.34	0.36
<b>Information score</b>	<b>Value</b>			
$I_{PPE}$	1.67	1.57	1.70	1.58
$I_{EEPAS}$	2.15	1.86	2.29	2.02
$\Delta I^*$	0.48	0.29	0.59	0.44

$$* \Delta I = I_{EEPAS} - I_{PPE}$$

### 3.4.2 Interface earthquakes

There are 21 interface earthquakes in the target set. Table 3 shows the result of fitting the models to these data for different predictor sets of earthquakes.

The highest value of  $I_{PPE}$  (2.27) is attained when the predictor set consists of the interface and shallow ( $h \leq 45$  km) slab earthquakes. This indicates that large interface earthquakes tend to occur where large earthquakes have previously occurred either on the interface or in the shallow part of the slab, and the very high value of  $I_{PPE}$  (2.27), larger than comparable values in Tables 1 and 2, indicates that this tendency is a strong one.

The largest value of  $I_{EEPAS}$  (2.62) is attained when the predictor set consists of interface events only. This indicates that the precursory earthquakes for interface events nearly all occur on the interface itself. Again, this value is higher than any comparable values in Tables 1 and 2, indicating that the overall predictability of interface events is relatively high.

Comparing the fitted parameter values for the optimal model in Table 3 with those in Table 1, we note that  $a_M$  is larger (1.60 compared to 1.47),  $a_T$  is smaller (1.21 compared to 1.43),  $\sigma_A$  is much larger (2.03 compared to 1.06), and  $\mu$  is much smaller (0.12 compared to 0.5). The larger value of  $a_M$  indicates that precursor earthquakes tend to be relatively small in magnitude. Taking into account the difference for  $a_M$ , the differences for  $a_T$  and  $\sigma_A$  indicate that on average precursor times are relatively short and precursor areas relatively

large for earthquakes on the interface compared with those for earthquakes in general. Also, the relatively low value of  $\mu$  indicates that a high proportion of the large earthquakes on the interface have precursor sequences conforming well to the fitted parameters.

Table 3 Parameters and information scores for EEPAS model fitted to interface earthquakes in the Japan catalogue ( $N = 21$ ). EEPAS parameters not listed are constrained to the same values as in Table 1.

	<b>Predictor set</b>					
	Interface	Crust +interface	Interface +slab	Interface +slab ( $h \leq 45$ )	Crust +interface +slab	Crust +interface +slab ( $h \leq 45$ )
<b>Parameter</b>	<b>Fitted values</b>					
$a_M$	1.60	1.00	1.01	1.60	1.00	1.00
$a_T$	1.21	1.30	0.90	1.02	1.36	1.36
$\sigma_A$	2.03	1.59	2.77	2.46	1.95	1.75
$\mu$	0.12	0.36	0.50	0.37	0.50	0.50
<b>Information Score</b>	<b>Value</b>					
$I_{PPE}$	2.07	1.86	2.11	2.27	2.05	2.13
$I_{EEPAS}$	2.62	2.06	2.14	2.45	1.99	2.13
$\Delta I^*$	0.55	0.20	0.03	0.18	-0.06	0.00

$$* \Delta I = I_{EEPAS} - I_{PPE}$$

The results in Table 3 suggest that an EEPAS model which uses the PPE model derived from interface and shallow slab earthquakes, and precursory earthquakes from the interface only should provide a slightly better fit to the data than any model in Table 3. Such a model is considered in Table 4. The information score  $I_{EEPAS}$  is 2.62, actually slightly greater than that in the first column of Table 3 but by a negligible amount. Therefore, for simplicity, the model using interface only earthquakes for PPE and the time-varying component of EEPAS is preferred. However, the value of  $\Delta I$  from Table 4 is the best estimate of the time-varying information in the model.

Table 4 Parameters and information scores for EEPAS model fitted to interface earthquakes in the Japan catalogue ( $N = 42$ ). The PPE model is derived using interface and shallow slab earthquakes. The time-varying component of EEPAS is derived from interface earthquakes only.

<b>Parameter</b>	<b>Fixed or fitted values</b>
$a_M$	1.60
$a_T$	1.16
$\sigma_A$	2.13
$\mu$	0.50
<b>Information score</b>	<b>Value</b>
$I_{PPE}$	2.27
$I_{EEPAS}$	2.62
$\Delta I = I_{EEPAS} - I_{PPE}$	0.35

### 3.4.3 Crustal Earthquakes

There are 42 crustal earthquakes in the target set. Table 5 shows the result of fitting the models to these data for different predictor sets of earthquakes. We optimise the same four EEPAS parameters as in the previous section, with other parameters fixed to the same values listed in Table 1.

First, note that the  $I_{EEPAS}$  values are generally lower in Table 5 than in Table 1, indicating that large earthquakes in the crust are not as predictable on average as earthquakes in general in this region.

The highest value of both  $I_{EEPAS}$  and  $I_{PPE}$  is attained when the crust and interface earthquakes are used as the predictor set.

The PPE model fits better when the interface and crustal earthquakes are used as predictors, as indicated by the increase in the  $I_{PPE}$  value from 0.89 when crustal earthquakes alone are used, to 1.06 when crustal and interface earthquakes are used. Note also that every predictor set including the interface earthquake gives a higher value of  $I_{PPE}$  than every predictor set that excludes them. We infer from this result that Although the maximum value of  $I_{EEPAS}$  is attained when the interface and crustal earthquakes are used as predictors, the increase in  $I_{EEPAS}$  from 1.05 to 1.15 when the interface earthquakes are used is smaller than the corresponding increase for the PPE model. Since, with  $\mu = 0.5$ , the PPE model makes a 50% contribution to the EEPAS rate density, much of the increase in the  $I_{EEPAS}$  value can be attributed to the increase in  $I_{PPE}$ . Therefore, it should not be concluded that a significant proportion of the precursory earthquakes occur on the interface. The  $\Delta I$  value ( $I_{EEPAS} - I_{PPE}$ ) is 0.16 when crustal earthquakes alone are used as predictors, and only 0.11 when crustal and interface earthquakes are used.

It is clear from Table 2 that there is no benefit to the EEPAS model information score from including the slab earthquakes, and particularly the deeper events with  $45 < h \leq 120$  km, in the predictor set. Therefore, we can draw the conclusion that not many precursors to crustal earthquakes occur in the slab.

Table 5 Parameters and information scores for EEPAS model fitted to crustal earthquakes in the Japan catalogue ( $N = 42$ ). EEPAS parameters not listed are constrained to the same values as in Table 1.

	<b>Predictor set</b>					
	Crust	Crust +interface	Crust +slab	Crust +slab ( $h \leq 45$ )	Crust +interface +slab	Crust +interface +slab ( $h \leq 45$ )
<b>Parameter</b>	<b>Fitted values</b>					
$a_M$	1.25	1.27	1.18	1.26	1.27	1.27
$a_T$	1.51	1.48	1.46	1.48	1.46	1.46
$\sigma_A$	1.35	1.38	1.17	1.34	1.21	1.21
$\mu$	0.50	0.50	0.50	0.44	0.50	0.50
<b>Information score</b>	<b>Value</b>					
$I_{PPE}$	0.89	1.06	0.89	0.88	1.02	0.99
$I_{EEPAS}$	1.05	1.15	0.97	1.05	1.03	1.08
$\Delta I$	0.16	0.09	0.08	0.17	0.01	0.07

$$* \Delta I = I_{EEPAS} - I_{PPE}$$

To investigate further whether a significant proportion of precursory earthquakes to major crustal earthquakes occur on the plate interface, we fit an EEPAS model in which the PPE component is estimated using earthquakes from both the crust and interface, and the time-varying component is estimated using only the earthquakes from the crust. As well as the equal-weighting strategy adopted above, we also consider the alternative weighting strategy of down-weighting aftershocks. Increasing the number of fitted parameters from four to six, by optimising the parameters  $\sigma_M$  and  $\sigma_T$  is also considered, and the effect on the information score is examined. The results are summarised in Table 6.

For all four variations on the EEPAS model considered in Table 6, the value of  $I_{EEPAS}$  is greater than the maximum value in Table 5. The maximum value of  $I_{EEPAS}$  is attained for the case of down-weighted aftershocks and four free parameters. This is our preferred model for crustal earthquakes.

Table 6 Parameters and information scores for EEPAS model fitted to crustal earthquakes in the Japan catalogue ( $N = 42$ ). The PPE model is derived using crustal and interface earthquakes. The time-varying component of EEPAS is derived from crustal earthquakes only.

Parameter	Weighting strategy			
	Equal weights		Aftershocks down-weighted	
	Number of free parameters			
	4	6	4	6
<b>Fitted values</b>				
$a_M$	1.27	1.37	1.31	1.49
$\sigma_M$	0.32	0.50	0.32	0.50
$a_T$	1.49	1.45	1.45	1.38
$\sigma_T$	0.23	0.22	0.23	0.20
$\sigma_A$	1.29	1.16	1.41	1.29
$\mu$	0.50	0.49	0.50	0.50
<b>Information score</b>	<b>Value</b>			
$I_{PPE}$	1.06			
$I_{EEPAS}$	1.24	1.25	1.29	1.28
$\Delta I^*$	0.18	0.17	0.23	0.22

$$* \Delta I = I_{EEPAS} - I_{PPE}$$

### 3.5 Enhancement of information scores

The overall results of fitting the EEPAS model are summarised in Table 7, in which the information scores for the best model for each targeted subset of earthquakes are shown, together with those for the fit to all earthquakes without regard to tectonic type and those for the combined model consisting of the best model for each tectonic-type subset. It is notable that the overall information scores of the best models combined are higher than those for the model fitted to all data without regard to tectonic type: for  $I_{PPE}$  by 0.14, for  $I_{EEPAS}$  by 0.38 and for  $\Delta I$  by 0.24.

Table 7 Information scores for best model in each class and best combined model in fitting to the learning set (1966-1995).

Information score	Target set				
	All (N=105) without regard to tectonic type	Slab (N=42) best model	Interface (N=21) best model	Crust (N=42) best model	All (N=105) best models combined
	Value				
$I_{PPE}$	1.42	1.70	2.27	1.06	1.56
$I_{EEPAS}$	1.58	2.29	2.62	1.29	1.96
$\Delta I^*$	0.16	0.59	0.35	0.23	0.40

$$* \Delta I = I_{EEPAS} - I_{PPE}$$

#### 4.0 TESTS ON INDEPENDENT DATA

For testing on independent data the information score  $I_M$  for a model  $M$  is defined as

$$I_M = (\ln L_M - \ln L_{SUP}) / N \quad (3)$$

where  $\ln L$  is the log likelihood statistic and  $N$  is the number of target earthquakes in the testing set. The number of fitted parameters does not affect the information score for independent testing because the parameter values are all fixed at the testing stage.

Fitted models described in the previous section were applied to the testing set of earthquakes (1996 – 2005) and the information scores were computed. These testing results are summarised in Table 8, in which the information scores for the best model for each targeted subset of earthquakes are shown, together with those for the model for all earthquakes without regard to tectonic type and those for the combined model consisting of the best model for each tectonic-type subset.

Overall, the test on independent data confirms the increased information value of the new combined model.

Table 8 Information scores for best model in each class and best combined model evaluated on the testing set of earthquakes (1996-2005).

Information score	Target set				
	All (N=37) without regard to tectonic type	Slab (N=13) best model	Interface (N=7) best model	Crust (N=17) best model	All (N=37) best models combined
$I_{PPE}$	1.07	1.90	2.42	0.38	1.30
$I_{EEPAS}$	1.29	2.07	2.69	1.05	1.72
$\Delta I^*$	0.22	0.17	0.27	0.67	0.42

$$*\Delta I = I_{EEPAS} - I_{PPE}$$

The likelihood scores in Table 8 can be compared to those in Table 7. It is noticeable that, unlike Table 7, the value of  $\Delta I$  in Table 8 is higher for the crust than for the interface or slab subsets. The high value for the crust is due to a particularly low value of  $I_{PPE}$  rather than a high value of  $I_{EEPAS}$ . Conversely, the relatively low values of  $\Delta I$  for the slab and interface appear to be due to high values of  $I_{PPE}$  rather than to low values of  $I_{EEPAS}$ . In any case, not too much reliance should be placed on the results for the individual subsets because of the relatively small number of target earthquakes in each. But it is notable that in Table 8, as in Table 7, the overall information scores of the best models combined are higher than those for the model fitted to all data without regard to tectonic type, and by similar amounts: for  $I_{PPE}$  by 0.23, for  $I_{EEPAS}$  by 0.43 and for  $\Delta I$  by 0.20.

These increases are large enough so that their statistical significance is not in question. Statistical significance is generally achieved with an increase in the log likelihood of about 2 (e.g., Evison and Rhoades, 1999), which in this case corresponds to an increase in the information score of about 0.05.

The contribution that an earthquake makes to the likelihood is proportional to the rate density of earthquake occurrence at its time of occurrence, magnitude and location. In Table 9, this rate density is given for each earthquake in the testing set for the SUP, PPE and EEPAS models which take tectonic type into account. The rate densities tabulated are normalised

relative to a reference (RTR) rate density in which one earthquake per year of magnitude  $m$  or greater occurs in an area of  $10^m \text{ km}^2$ . They show that for both the PPE and EEPAS models the normalised rate density varies over several orders of magnitude.

More detail of the variation of the earthquake occurrence rate density for six major crustal earthquakes in the test period is given in Figures 9 – 14. In these figures, the normalized rate density of earthquake occurrence under the EEPAS model is plotted as a function of location for fixed time and magnitude, as a function of time for fixed magnitude and location, and as a function of magnitude for fixed location and time, where the fixed values in each case are the coordinates of the major earthquake.

The Tottori earthquake (Figure 9) and the Niigata-ken Chuetsu earthquake (Figure 10) are examples for which the EEPAS model worked well. For each of these events, the rate density is much higher under the EEPAS model than under the PPE model (Table 9). Also, the location of the earthquake is near to a local maximum of the spatial plot, the time plot shows a rising rate density leading up to the time of the earthquake, and the magnitude of the earthquake is near to maximum of the rate density versus magnitude plot. Note that the sudden increase in the rate density immediately following the earthquake is due the PPE component of the model, in which the rate density increases when the major earthquake is incorporated into the data defining the model.

The West off Fukuoka earthquake (Figure 11) and the Noto-hanto-oki earthquake (Figure 12) are examples for which the EEPAS model did not work well. For the West off Fukuoka event the rate density is much lower under the EEPAS model than under the PPE model (Table 9). The Noto-hanto-oki earthquake is beyond the end of the present catalogue and so is not shown in Table 9, but for it also the rate density is low under the EEPAS model, and it is evident from Figure 12 that the EEPAS rate density consists mainly of its PPE component. For these earthquakes, the location of the earthquake is nowhere near to a local maximum of the spatial plot, the time plot is flat leading up to the time of the earthquake, and the normalised rate density versus magnitude plot is also flat. The latter two features indicate that the time-varying component of the EEPAS model contributes hardly anything to the rate density in the vicinity of these earthquakes.

The Niigata-Ken Chuetsu-oki earthquake (Figure 13) and the Iwate-Miyagi Nairiku earthquake (Figure 14) are examples which fall between the extremes of the previously discussed pairs of earthquakes. For these events the time-varying component of the EEPAS model provides some information, but the earthquakes are not close to the maximum of the rate density for all coordinates. The Niigata-Ken-Chuetsu-oki earthquake occurred in a shoulder region of the spatial plot where the rate density was moderately low, but the time plot shows that the rate density was increasing at the time of the earthquake and the magnitude is not far from a local maximum of the rate density. The Iwate-Miyagi Nairiku earthquake occurred near a local maximum of the spatial plot where the rate density was quite high. The time plot shows that rate density had been increasing from 2000 to 2005, but was tailing off at the time of the earthquake, and the magnitude plot shows that the earthquake magnitude was at a local minimum of the rate density.

It should be noted that the earthquake coordinates used in Figures 12 – 14 are taken from moment magnitude determinations and may differ from what will eventually be recorded in the SEIS-PC catalogue.

## EEPAS M7.3 2000/10/ 6

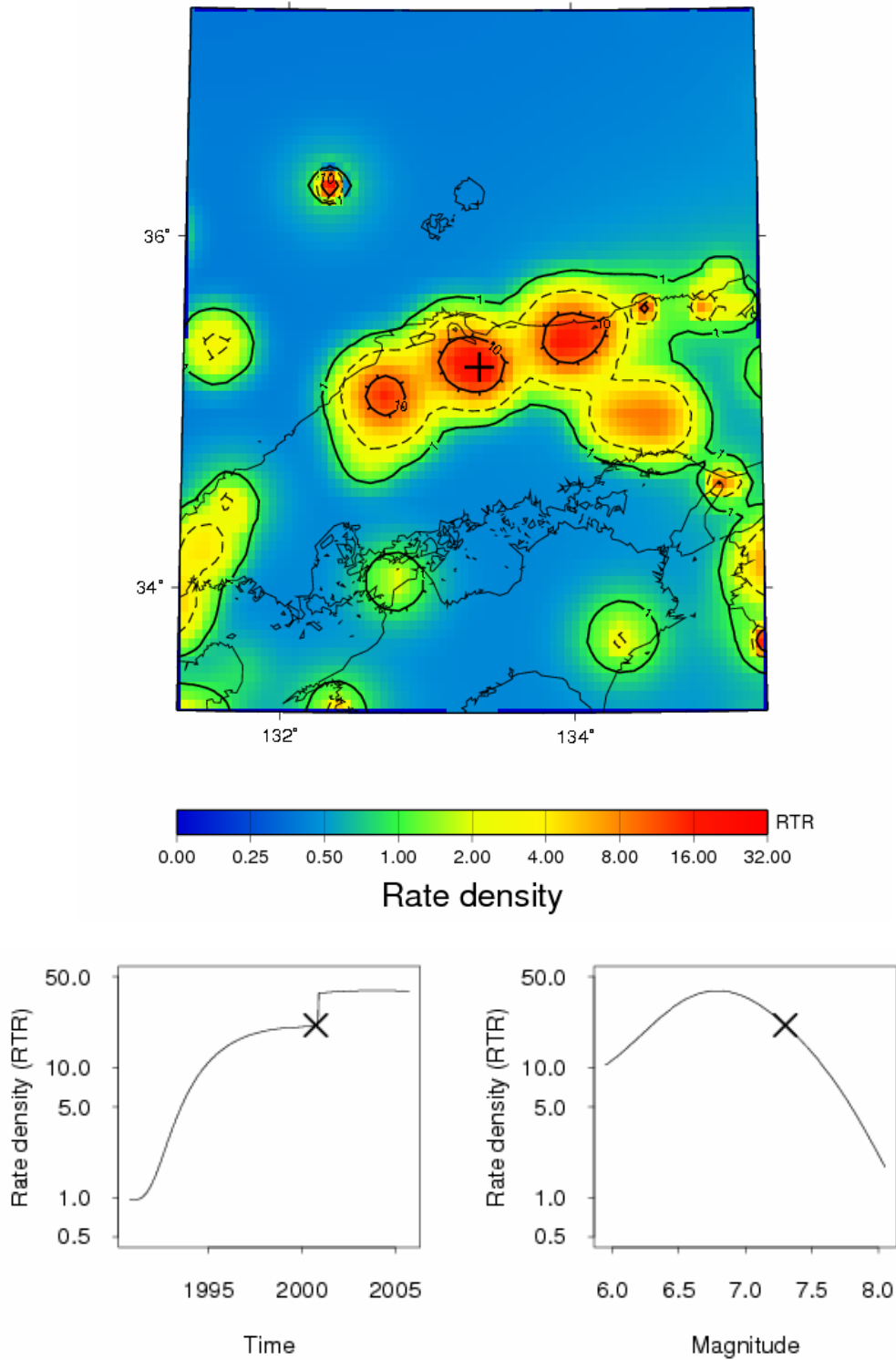


Figure 9 Normalized rate density (RTR) of earthquake occurrence under the EEPAS model as a function of location (upper), as a function of time (lower left) and as a function of magnitude (lower right). The fixed values are those of the Tottori earthquake of 2000 10 06. The location, time and magnitude of this earthquake are marked on the respective figures.

# EEPAS M6.8 2004/10/23

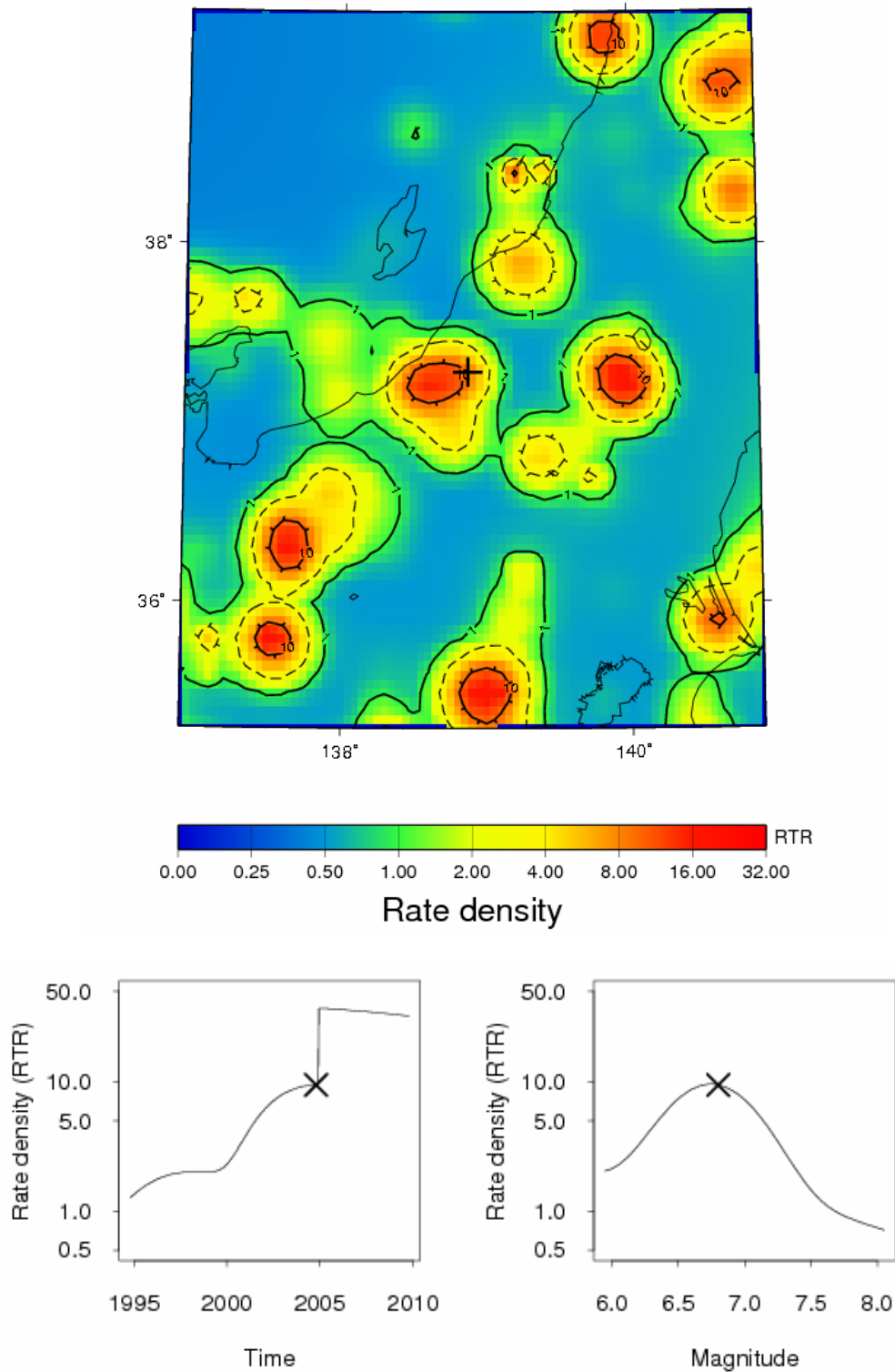


Figure 10 Normalized rate density (RTR) of earthquake occurrence under the EEPAS model as a function of location (upper), as a function of time (lower left) and as a function of magnitude (lower right). The fixed values are those of the Niigata-ken-Chuetsu earthquake of 2004 10 06. The location, time and magnitude of this earthquake are marked on the respective figures.

## EEPAS M7.0 2005/ 3/20

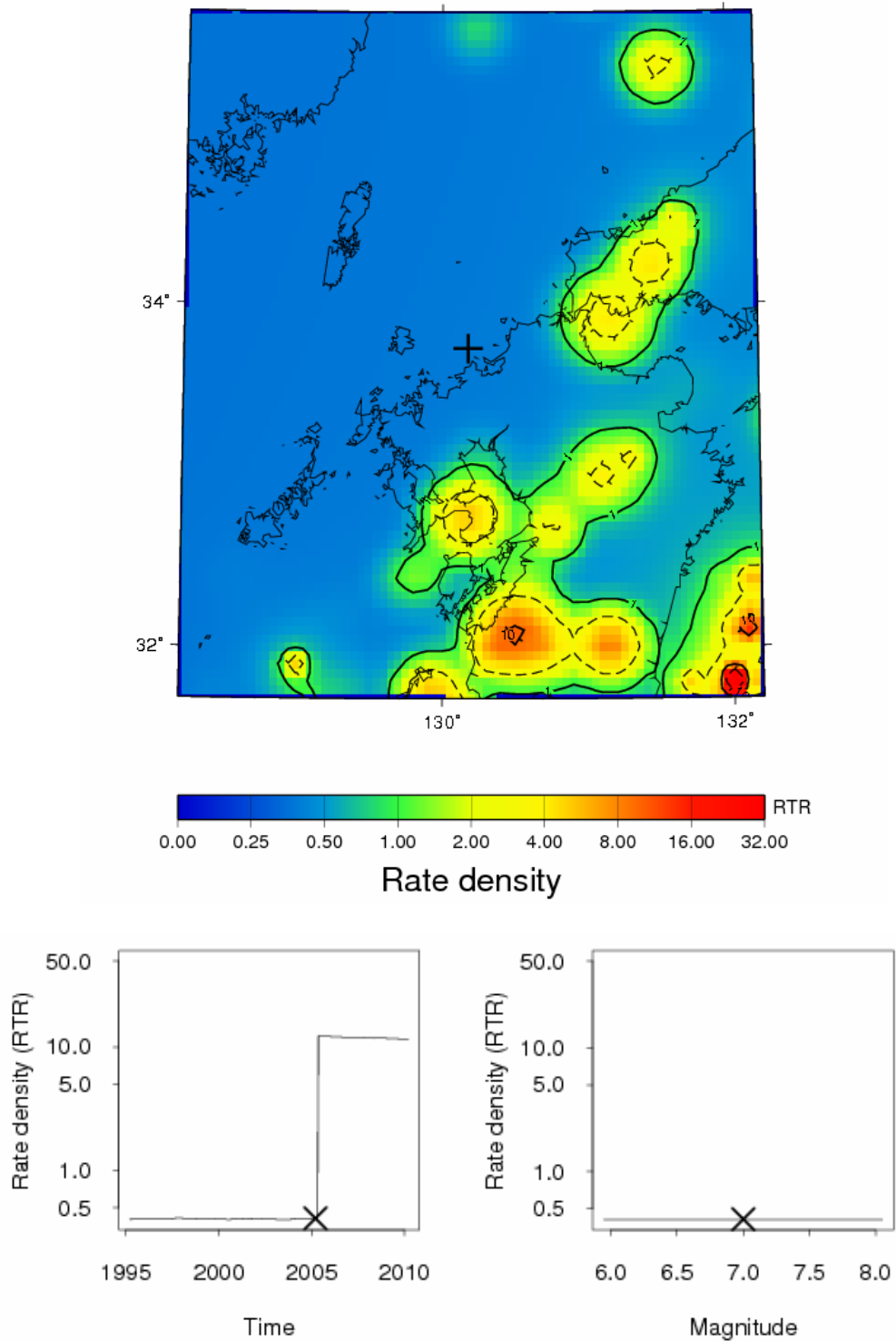


Figure 11 Normalized rate density (RTR) of earthquake occurrence under the EEPAS model as a function of location (upper), as a function of time (lower left) and as a function of magnitude (lower right). The fixed values are those of the West off Fukuoka earthquake of 2005 03 20. The location, time and magnitude of this earthquake are marked on the respective figures.

## EEPAS M6.7 2007/ 3/25

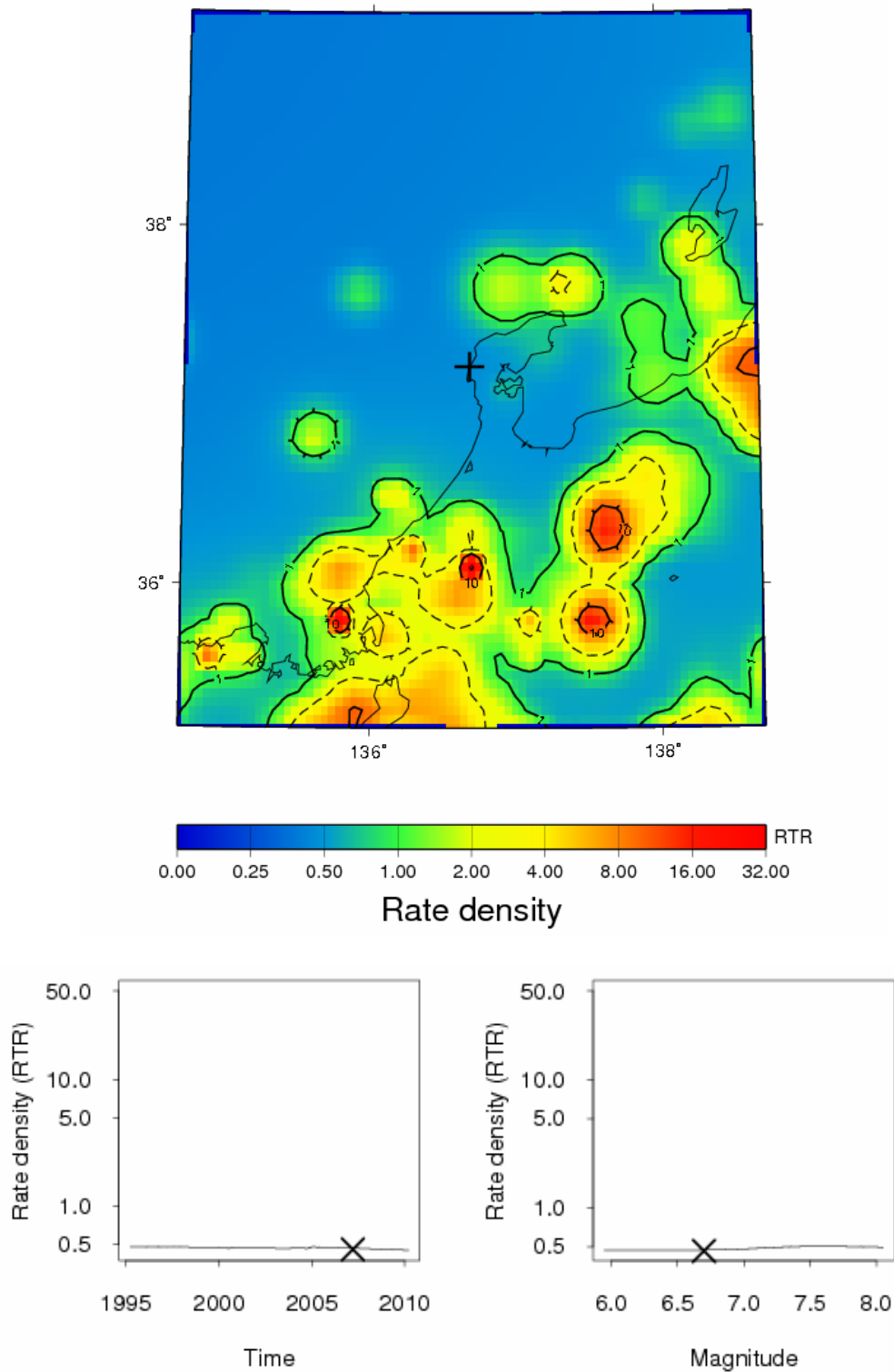


Figure 12 Normalized rate density (RTR) of earthquake occurrence under the EEPAS model as a function of location (upper), as a function of time (lower left) and as a function of magnitude (lower right). The fixed values are those of the Noto-hanto-oki earthquake of 2007 03 25. The location, time and magnitude of this earthquake are marked on the respective figures.

# EEPAS M6.6 2007/ 7/16

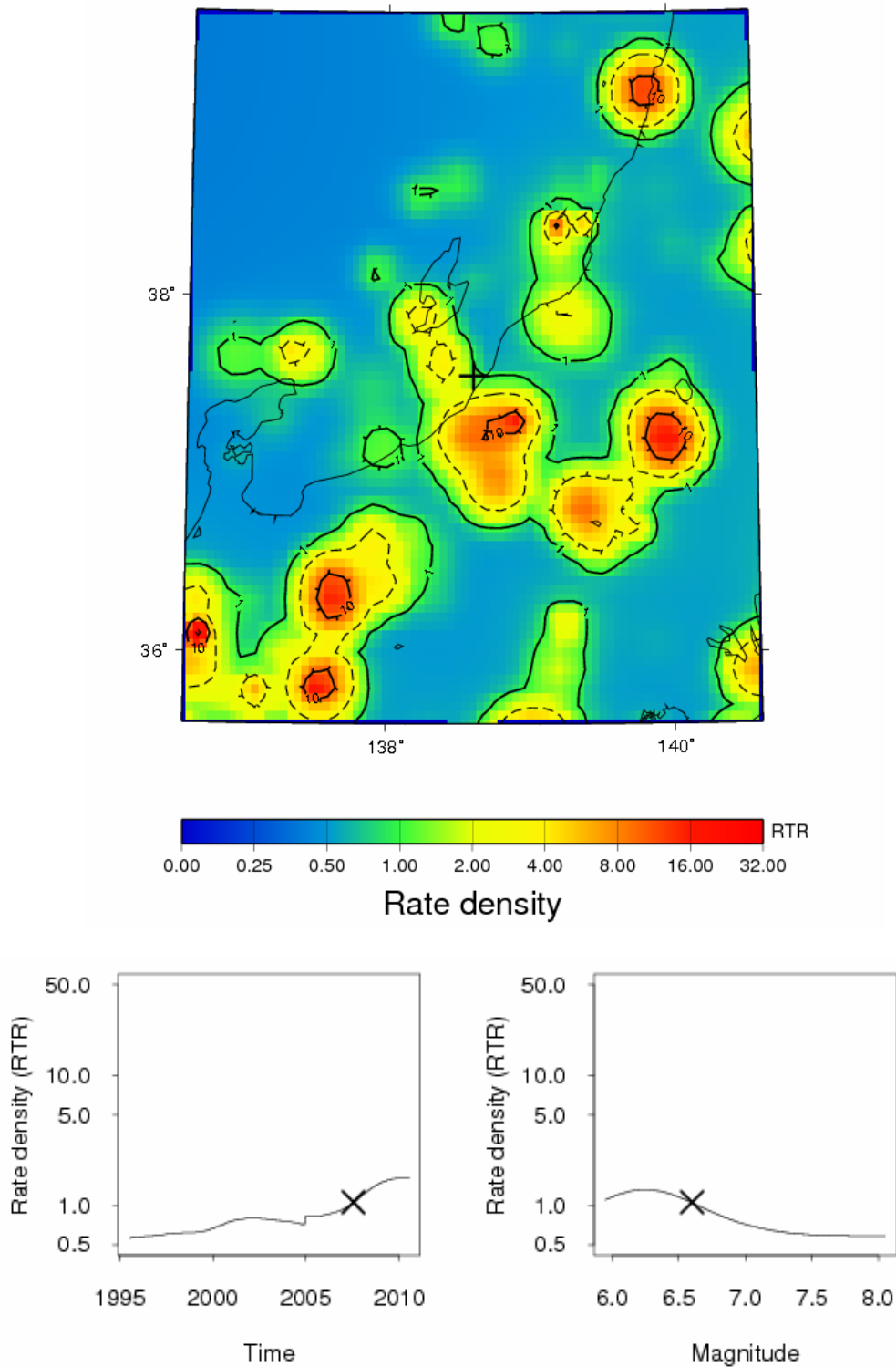


Figure 13 Normalized rate density (RTR) of earthquake occurrence under the EEPAS model as a function of location (upper), as a function of time (lower left) and as a function of magnitude (lower right). The fixed values are those of the Niigata-ken Chuetsu-oki earthquake of 2007 07 16. The location, time and magnitude of this earthquake are marked on the respective figures.

# EEPAS M6.9 2008/ 6/14

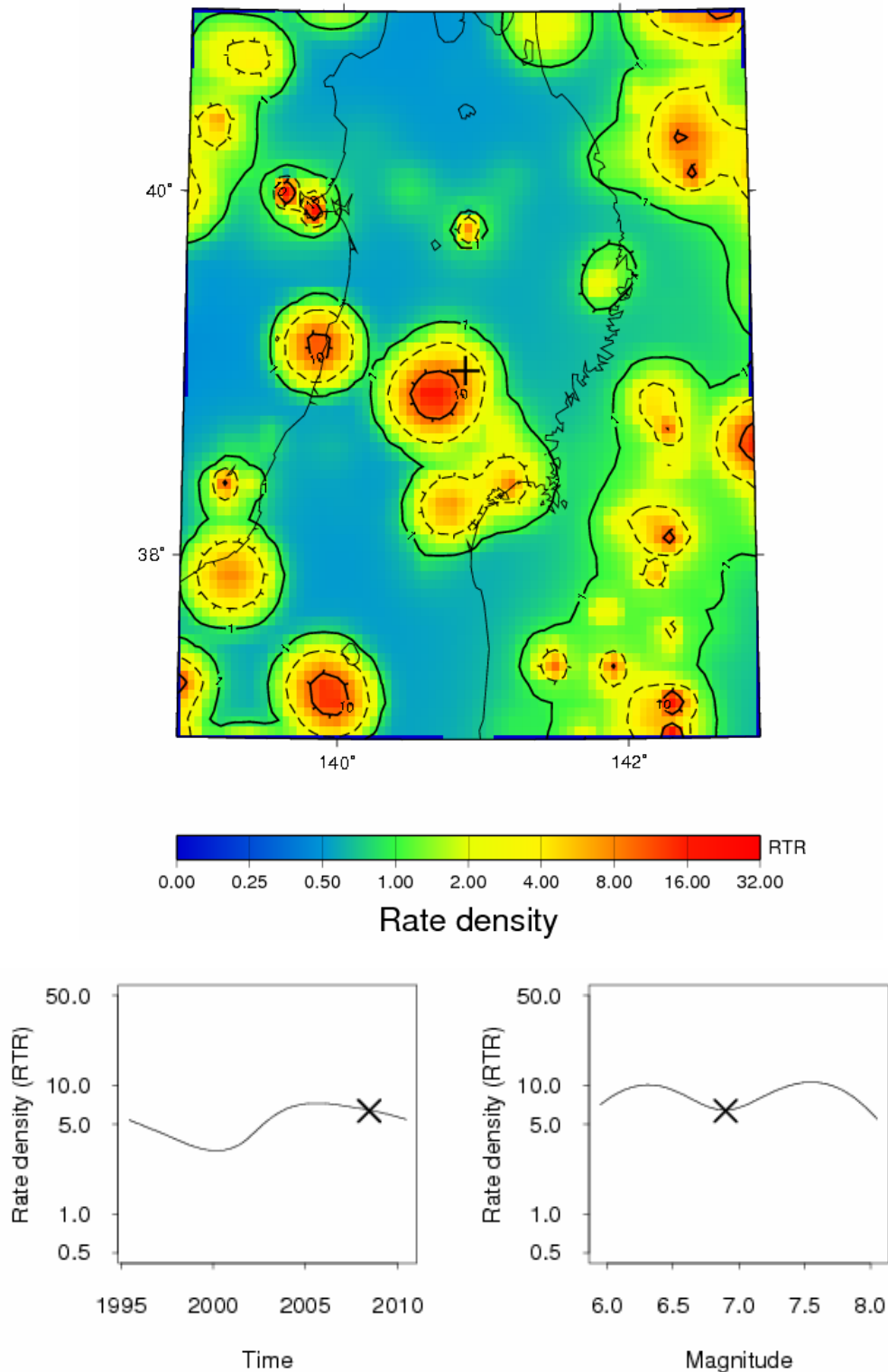


Figure 14 Normalized rate density (RTR) of earthquake occurrence under the EEPAS model as a function of location (upper), as a function of time (lower left) and as a function of magnitude (lower right). The fixed values are those of the Iwate-Miyagi earthquake of 2008 06 14. The location, time and magnitude of this earthquake are marked on the respective figures.

The range of possible outcomes illustrated in these examples must of course be allowed for when interpreting EEPAS forecasts for risk mitigation or other practical purposes. Despite the overall success of the model in providing improved time-varying estimates of earthquake occurrence rate, large earthquakes will occasionally occur at times, magnitudes and locations where the rate density is rather low. Another factor to be considered is that even when the rate density is highest, the hazard is still low enough that large earthquakes are far less likely than not to occur over short time periods of a few years within small regions of a few hundred km<sup>2</sup>.

Table 9 Earthquakes (M > 5.95) in the region of surveillance during the test period, 1996-2005, and normalised rate densities under the SUP, PPE and EEPAS models taking tectonic type into account.

Date (y m d)	Location (Lat. Long.)	Magnitude	$\lambda_{SUP}$ (RTR)	$\lambda_{PPE}$ (RTR)	$\lambda_{EEPAS}$ (RTR)
<b>Slab</b>					
1996 02 17	37.31 142.55	6.8	0.81	3.54	1.43
1996 09 11	35.64 141.22	6.4	0.81	7.39	8.31
2000 06 03	35.69 140.75	6.1	0.81	5.37	24.91
2000 07 21	36.53 141.12	6.4	0.81	7.67	14.39
2001 03 24	34.13 132.69	6.7	0.81	0.19	0.07
2002 10 14	41.15 142.28	6.1	0.81	2.61	16.36
2002 11 03	38.90 142.14	6.3	0.81	32.54	19.99
2003 05 26	38.82 141.65	7.1	0.81	1.66	0.57
2003 10 31	37.83 142.70	6.8	0.81	17.46	17.59
2005 04 11	35.73 140.62	6.1	0.81	3.22	15.44
2005 07 23	35.58 140.14	6.0	0.81	3.18	13.26
2005 10 19	36.38 141.04	6.3	0.81	30.9	46.25
2005 12 02	38.07 142.35	6.6	0.81	16.18	5.53
<b>Interface</b>					
1996 10 19	31.80 132.01	6.9	0.44	245.63	96.66
2000 06 25	31.04 131.63	6.0	0.44	0.29	3.54
2000 10 03	40.17 143.37	6.0	0.44	2.87	9.98
2003 04 08	36.37 141.96	6.0	0.44	2.33	1.50
2005 08 16	38.15 142.28	7.2	0.44	6.87	4.92
2005 08 24	38.44 143.09	6.3	0.44	2.61	2.38
2005 12 17	38.45 142.18	6.1	0.44	8.34	5.53
<b>Crust</b>					
1996 08 11	38.91 140.63	6.1	1.06	1.17	5.05
1996 12 03	31.77 131.68	6.7	1.06	1.77	2.80
1997 03 26	31.97 130.36	6.6	1.06	0.88	0.69
1997 05 13	31.95 130.30	6.4	1.06	0.87	0.51
1997 05 24	34.50 137.50	6.0	1.06	1.11	0.59
1997 06 25	34.44 131.67	6.6	1.06	1.26	1.00
1998 09 03	39.81 140.90	6.2	1.06	1.12	1.82
2000 07 15	34.42 139.24	6.3	1.06	1.91	43.75
2000 10 06	35.27 133.35	7.3	1.06	0.95	21.24
2001 08 14	41.00 142.44	6.4	1.06	2.97	3.49
2003 07 26	38.40 141.17	6.4	1.06	1.25	0.64
2004 10 23	37.29 138.87	6.8	1.06	1.21	9.47
2004 10 23	37.35 138.98	6.3	1.06	1.12	1.89
2004 10 23	37.25 138.83	6.0	1.06	1.14	2.83
2004 10 23	37.31 138.93	6.5	1.06	1.33	4.85
2004 10 27	37.29 139.03	6.1	1.06	1.34	1.16
2005 03 20	33.74 130.18	7.0	1.06	0.82	0.41

For illustration purposes, sample forecast maps of EEPAS model rate densities for the whole of Japan are presented in Figures 15 – 21. These are for 30 June 2009 based on the earthquake catalogue up to the end of 2005. Because of the gap between the end of the catalogue and the forecast date, these maps are not as informative as they would be with a more up-to-date catalogue. The lack of earthquakes in the intervening period affects the lower magnitude forecasts (M6.5) the most and the high magnitude forecasts (M 8.0) the least. Figure 15 and 16 show the forecasts of earthquakes in the slab at magnitudes 6.5 and 7.0, respectively. Figures 17 and 18 show the forecasts of earthquakes on the plate interface at magnitudes 7.0 and 8.0, respectively. Figures 19 and 20 show the forecasts of earthquakes in the crust at magnitudes 6.5 and 7.0, respectively. And Figure 20 shows a combined forecast for earthquakes of all tectonic types at hypocentral depth  $h \leq 120$  km. To get a full picture of the EEPAS model forecasts at a given date, a set of similar maps covering the complete magnitude range of interest is required. However, the maps change gradually with magnitude level and slowly in time, with the forecasts at lower magnitude levels changing more rapidly.

## Slab EEPAS M6.5 2009/ 6/30

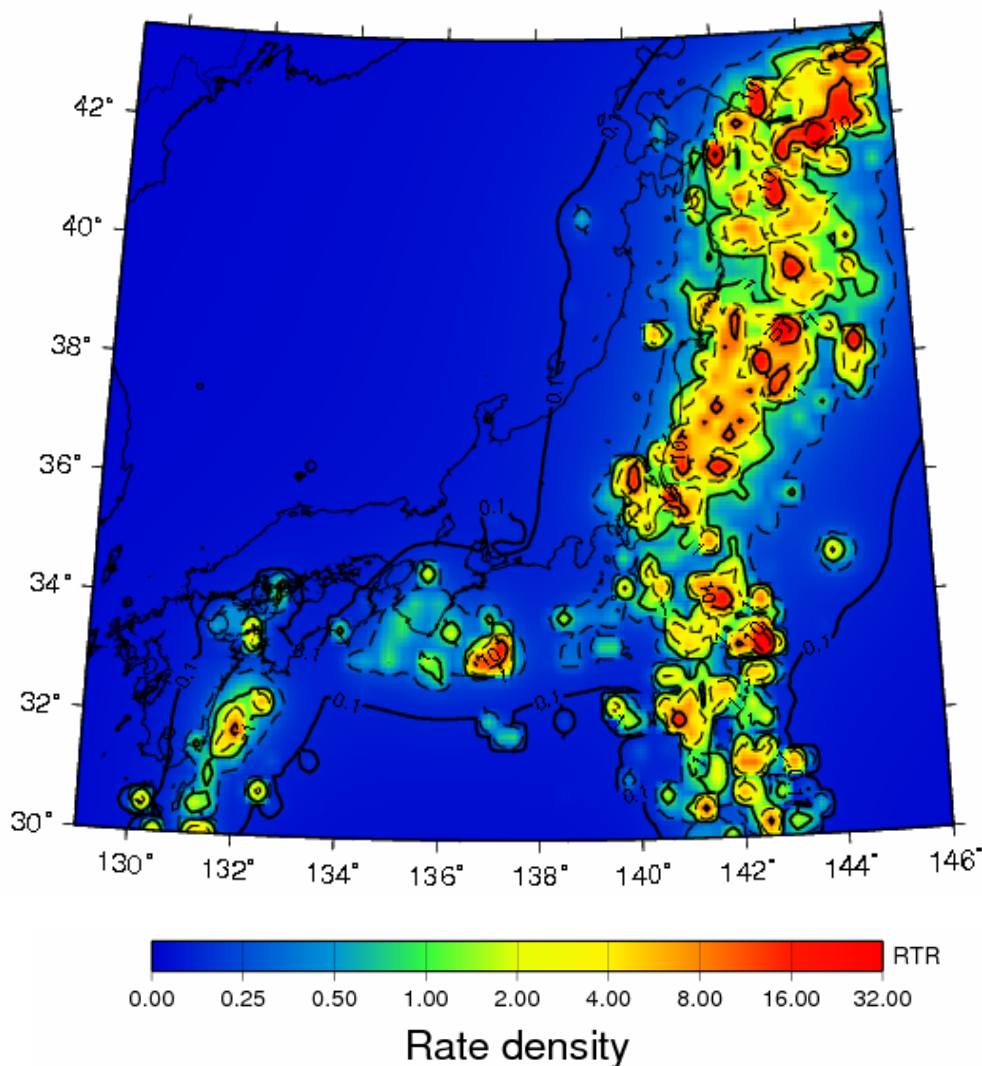


Figure 15 EEPAS model forecast of rate density of earthquake occurrence in the slab at hypocentral depth  $h \leq 120$  km for magnitude 6.5 on 2009 06 30, based on catalogue up to end of 2005.

# Slab EEPAS M7.0 2009/ 6/30

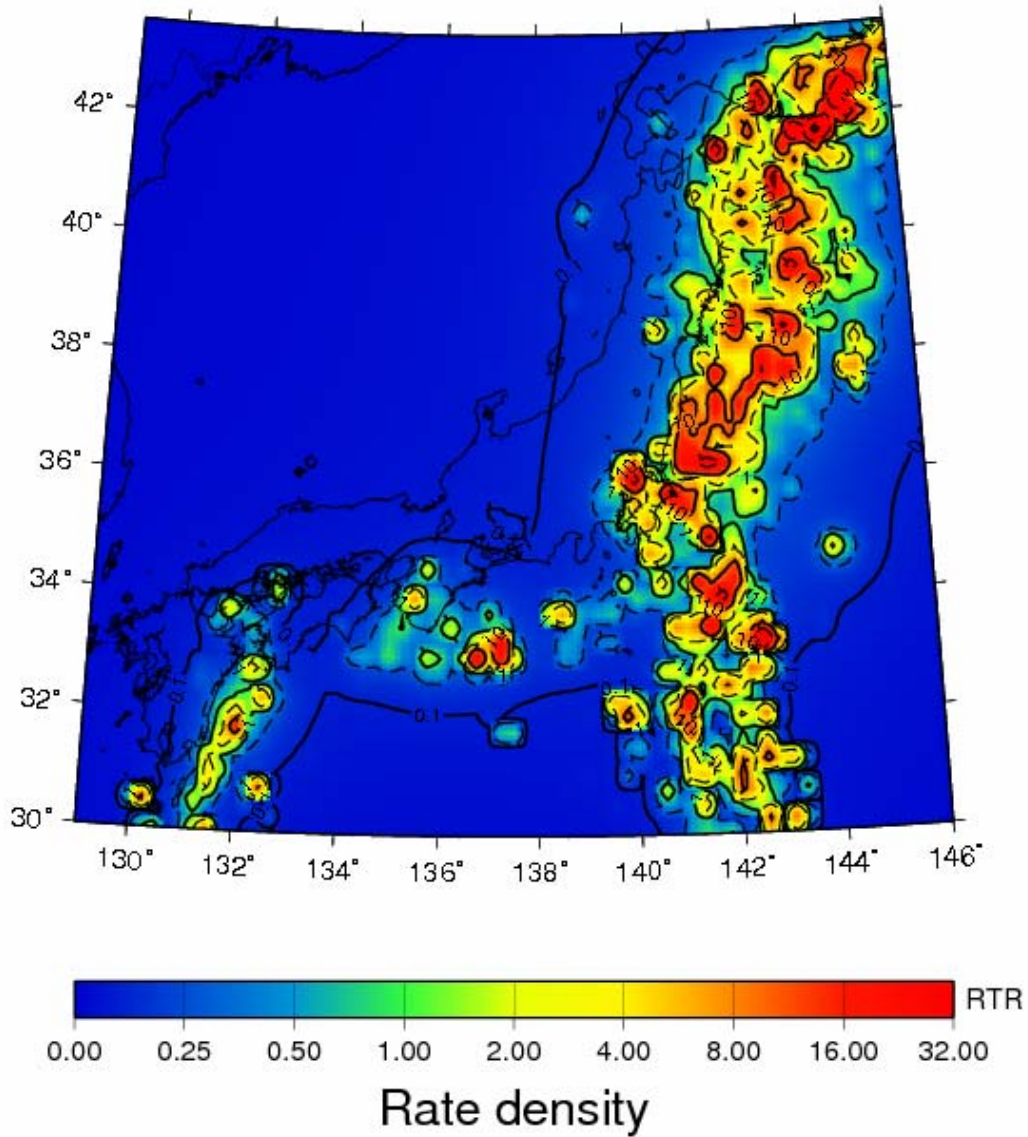


Figure 16 EEPAS model forecast of rate density of earthquake occurrence in the slab at depth  $h \leq 120$  km for magnitude 7.0 on 2009 06 30, based on catalogue up to end of 2005.

# Interface EEPAS M7.0 2009/ 6/30

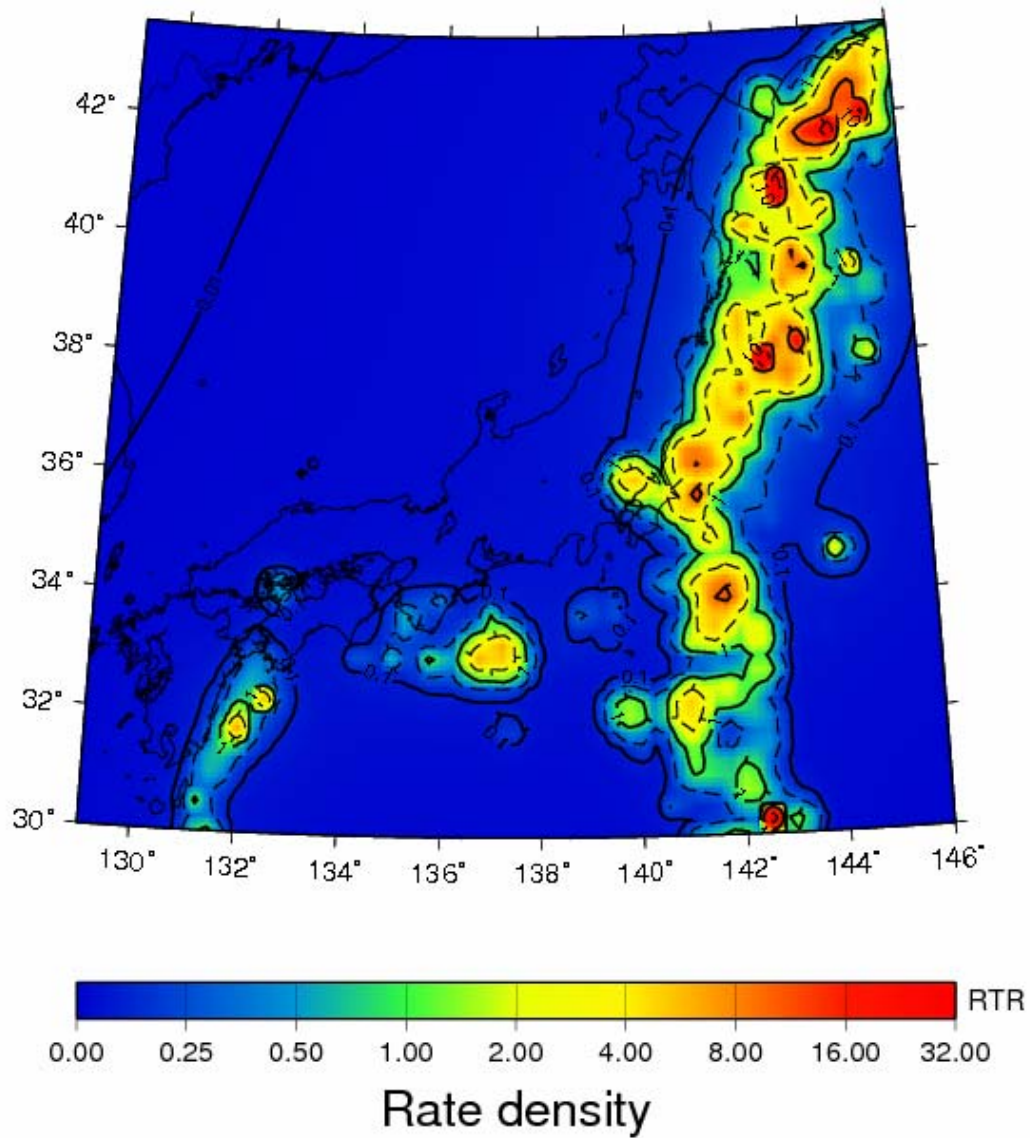


Figure 17 EEPAS model forecast of rate density of earthquake occurrence on the plate interface for magnitude 7.0 on 2009 06 30, based on catalogue up to end of 2005.

# Interface EEPAS M8.0 2009/ 6/30

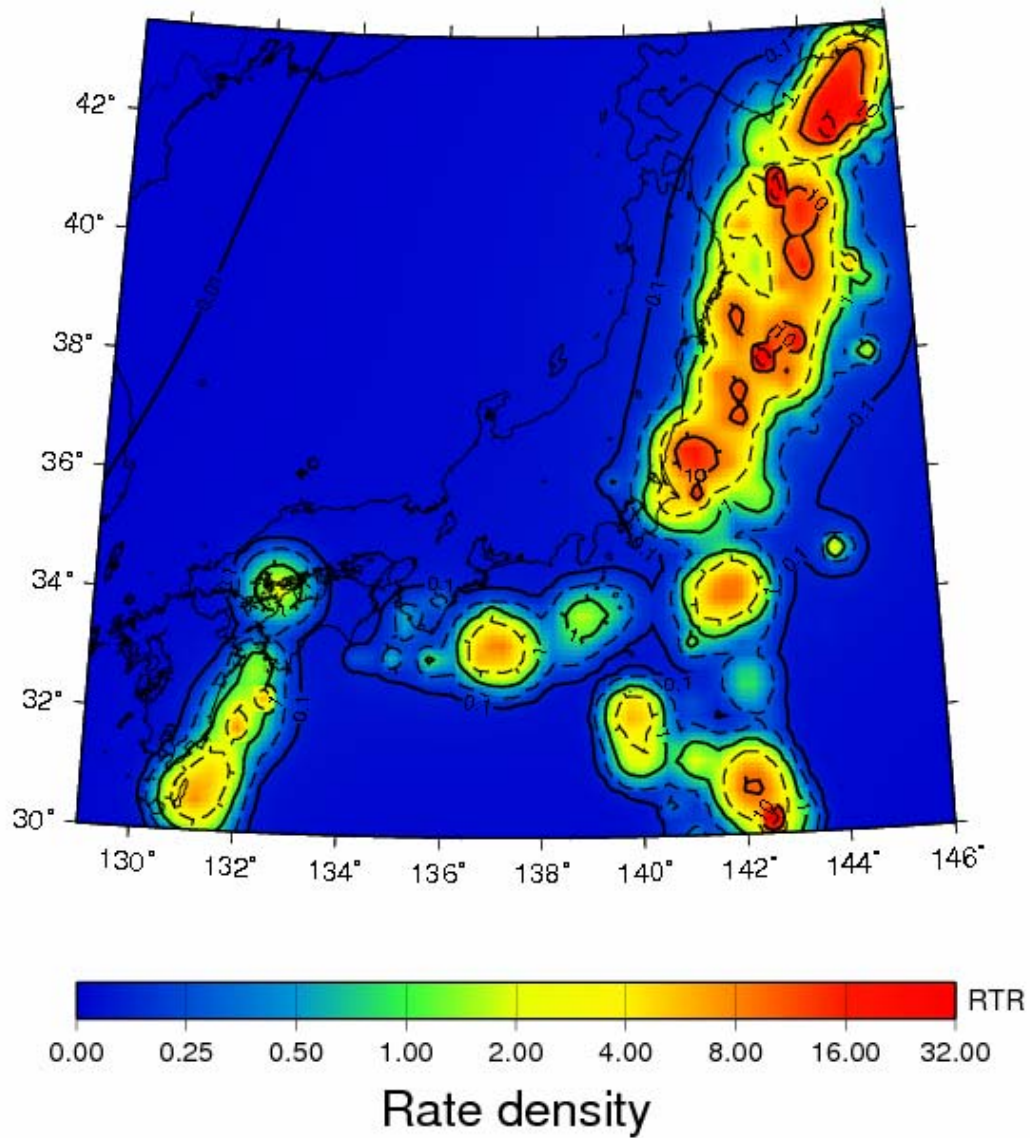


Figure 18 EEPAS model forecast of rate density of earthquake occurrence on the plate interface for magnitude 8.0 on 2009 06 30, based on catalogue up to end of 2005.

# Crust EEPAS M6.5 2009/ 6/30

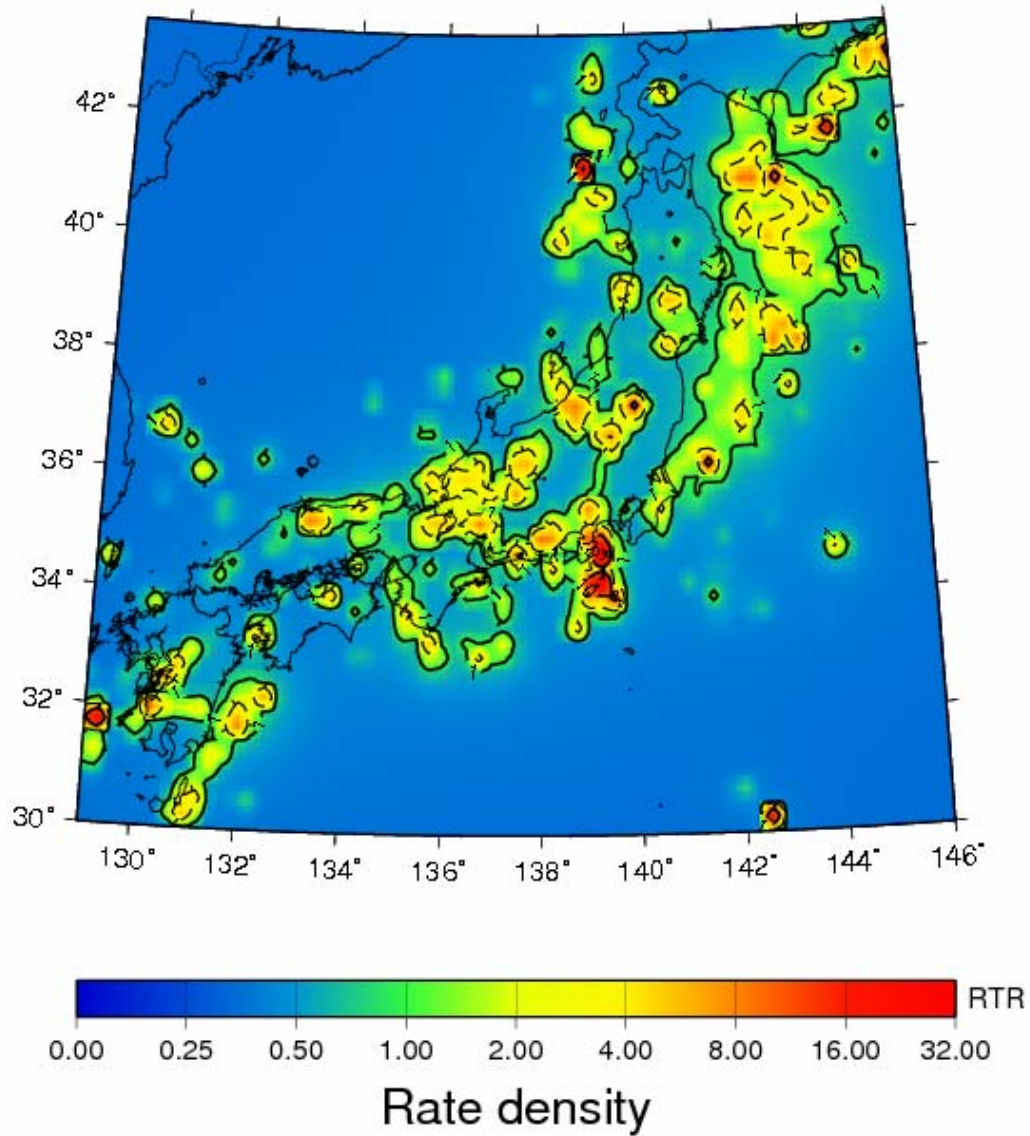


Figure 19 EEPAS model forecast of rate density of earthquake occurrence in the crust for magnitude 6.5 on 2009 06 30, based on catalogue up to end of 2005.

# Crust EEPAS M7.0 2009/ 6/30

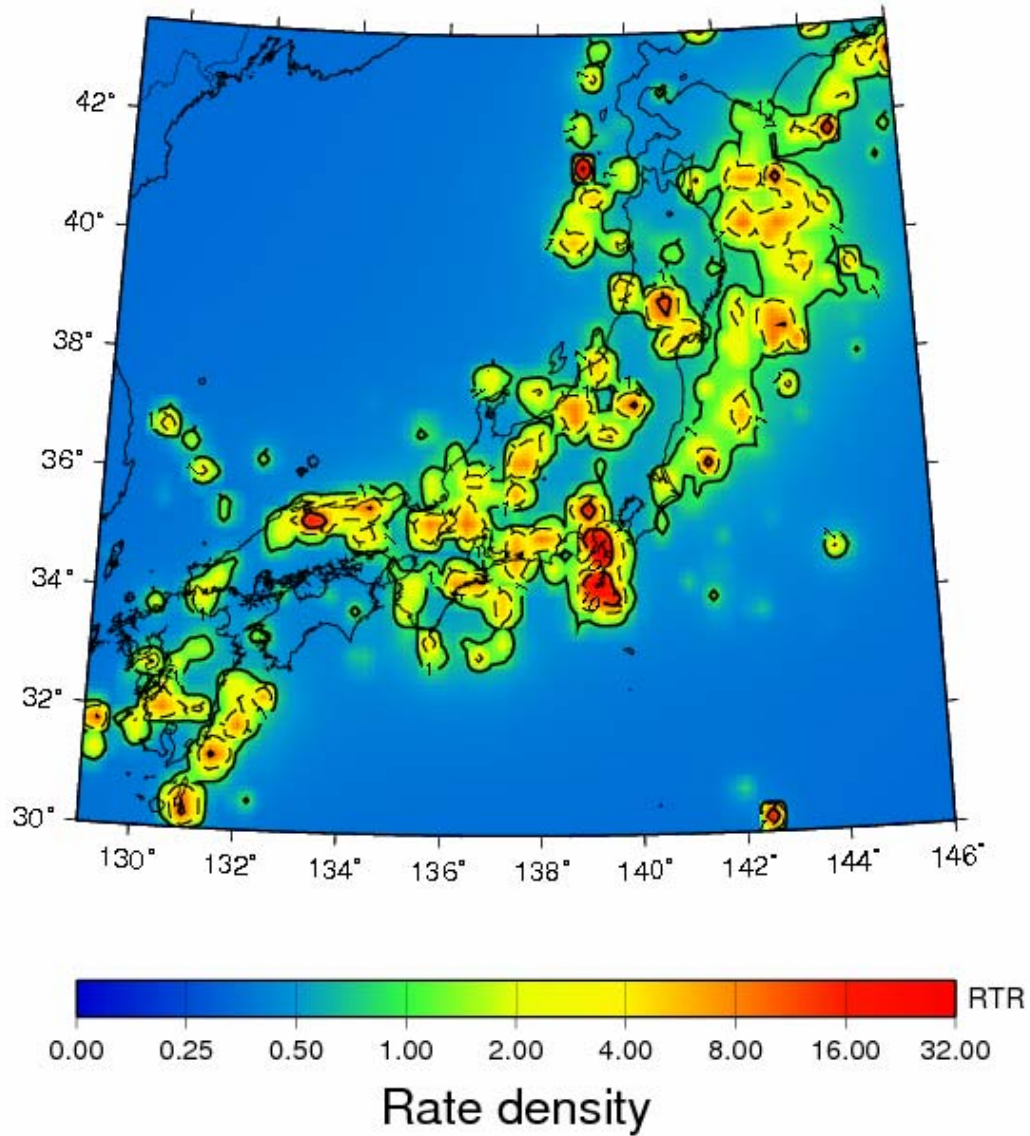


Figure 20 EEPAS model forecast of rate density of earthquake occurrence in the crust for magnitude 7.0 on 2009 06 30, based on catalogue up to end of 2005.

# Combined EEPAS M7.0 2009/ 6/30

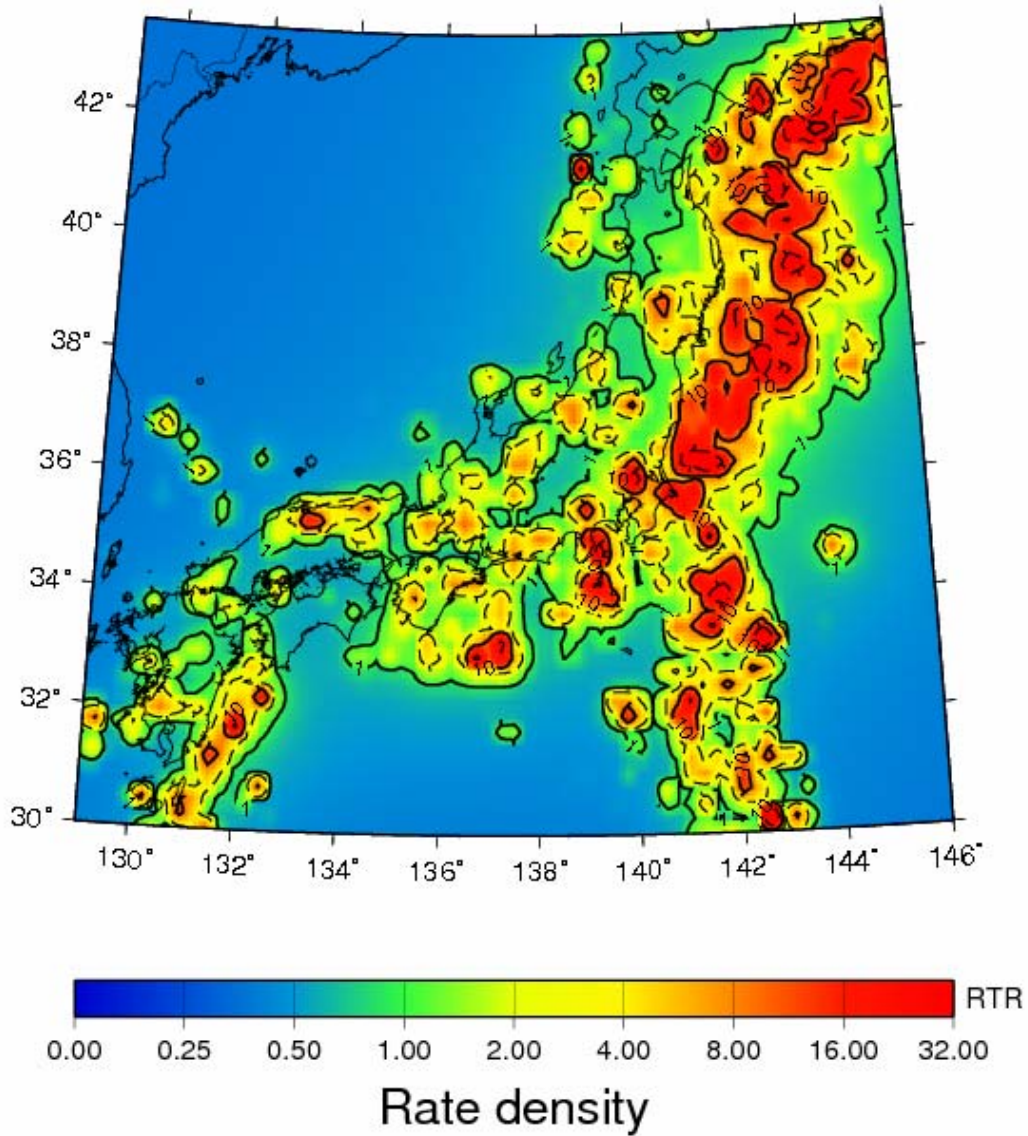


Figure 21 Combined EEPAS model forecast of rate density of earthquake occurrence at hypocentral depth  $h \leq 120$  km for magnitude 7.0 on 2009 06 30, based on catalogue up to end of 2005.

## 5.0 CONCLUSION

Distinguishing the three tectonic categories of earthquake has generally confirmed the hypothesis that earthquakes interactions are stronger between earthquakes of similar tectonic types than between those of different types, and has resulted in an improved forecasting model for the Japan region.

The analysis of earthquakes in the slab has shown that large earthquakes in the slab tend to occur near to where large earthquakes have previously occurred either in the slab or on the plate interface, and that the earthquakes precursory to large earthquakes in the slab may occur either in the slab or on the interface, but hardly ever in the crust.

Analysis of plate interface earthquakes has shown large interface earthquakes tend to occur where large earthquakes have previously occurred either on the interface or in the shallow part of the slab. Also, the precursory earthquakes for interface events nearly all occur on the interface itself.

Analysis of crustal earthquakes has shown that large earthquakes in the crust tend to occur near to where large earthquakes have previously occurred either in the crust or on the plate interface. Also, the precursory earthquakes for crustal events mainly occur in the crust.

Taking tectonic type into account, the optimal EEPAS model uses slab and interface events as precursors to major slab earthquakes, interface events only as precursors to major interface events, and crustal events only as precursors to major crustal events. For the smoothed-seismicity component of the EEPAS model, it is optimal to use slab and interface events to forecast the location of earthquakes in the slab, interface events only to forecast the location of earthquakes on the interface, and both crustal and interface events to forecast the location of events on the interface. The combined optimal models fit the learning data set data much better than an EEPAS model which does not take account of tectonic type, with the information score being increased by 0.38. The information score is higher for earthquakes in the slab and on the interface than for crustal earthquakes.

When the models were applied to the independent testing period, a similar overall information gain is obtained compared with a model which does not take account of tectonic type. A difference was that the information gain of the EEPAS model over the PPE model was much higher for crustal earthquakes than in the learning period.

A detailed analysis of six individual major crustal earthquakes in the testing period showed that the EEPAS forecast was quite informative for occurrence of the Tottori (2000) and Niigata-ken Chuetsu (2004) earthquakes, uninformative for the West off Fukuoka (2005) and Noho-hanto-oki (2007) earthquakes, and somewhat informative for the Niigata-ken Chuetsu-oki (2007) and Iwate-Miyagi (2008) earthquakes.

The Japan catalogue was used for this research because a plate interface model was available to readily separate it into tectonic categories and because the long instrumental record and high rate of earthquake occurrence facilitate statistical testing of the method. The results are highly relevant to New Zealand conditions because Japan has a similar tectonic environment, including subduction zones and large strike-slip faults. Therefore, it is likely that a similar improvement in forecasting performance could be obtained by applying these methods to the New Zealand catalogue.

## 6.0 ACKNOWLEDGEMENTS

This project was funded by the Earthquake Commission Research Foundation under project TVH 08/567. Rob Buxton and Mark Stirling have provided helpful reviews of the report.

## 7.0 REFERENCES

- Akaike, H. (1974). A new look at the statistical model identification, *IEEE Trans. Automatic Control AC-19*, 716-723.
- Console, R.; Murru, M. (2001). A simple and testable model for earthquake clustering. *Journal of Geophysical Research*, 106, 8699–8711.
- Console, R.; Murru, M.; Lombardi, A.M. (2003). Refining earthquake clustering models. *Journal of Geophysical Research*, 108, 2468, doi:10.1029/2002JB002130.
- Anderson, H.J. (1991). Focal mechanisms of some recent large New Zealand earthquakes. *NZ J. Geol. Geophys.*, 34, 103-109.
- Console, R.; Rhoades, D.A., Murru, M.; Evison, F.F.; Papadimitriou, E.E.; Karakostas, V.G. (2006). Comparative performance of time-invariant, long-range and short-range forecasting models on the earthquake catalogue of Greece. *Journal of Geophysical Research* 111, B09304, doi:10.1029/2005JB004113.
- Doser, D.I.; Webb, T.H. (2003). Source parameters of large historical (1917-1961) earthquakes, North Island, New Zealand. *Geophys. J. Int.*, 152, 795-832.
- Engdahl, E.R., R. vd. Hilst and R. Buland, (1998). Global teleseismic earthquake relocation with improved travel times and procedures for depth determination, *Bull. Seismol. Soc. Am.*, 88, 722-743.
- Evison, F.F. (1977). The precursory earthquake swarm. *Physics of the Earth and Planetary Interiors* 15, 19-23.
- Evison, F.F. (1982) Generalised precursory swarm hypothesis. *Journal of Physics of the Earth*, 30, 115-124.
- Evison, F.F.; Rhoades, D.A. (1993). The precursory earthquake swarm in New Zealand: hypothesis tests. *New Zealand Journal of Geology and Geophysics*, 36, 51-60.
- Evison, F.F.; Rhoades, D.A. (1997). The precursory earthquake swarm in New Zealand: hypothesis tests II. *New Zealand Journal of Geology and Geophysics*, 40, 537-547.
- Evison, F.F.; Rhoades, D.A. (1999). The precursory earthquake swarm in Japan: hypothesis test. *Earth Planets Space*, 51, 1267-1277.
- Evison, F.F.; Rhoades, D.A. (2000). The precursory earthquake swarm in Greece. *Ann. Geofis.*, 43, 991-1009
- Evison, F.F. and Rhoades, D.A. (2001). Model of long-term seismogenesis. *Ann. Geofis.*, 44(1), 81-93.

- Evison, F.F. and Rhoades, D.A. (2002). Precursory scale increase and long-term seismogenesis in California and northern Mexico. *Annals of Geophysics*, 45(3/4), 479-495.
- Evison, F.F.; Rhoades, D.A. (2004a) Demarcation and scaling of long-term seismogenesis. *Pure and applied geophysics*, 161(1): 21-45
- Evison, F.; Rhoades, D.A. (2004b) Long-term seismogenesis and self-organized criticality. *Earth, planets and space*, 56(8): 749-760
- Evison, F.F.; Rhoades, D.A. (2005) Multiple-mainshock events and long-term seismogenesis in Italy and New Zealand. *NZ J. Geol. Geophys.* 48 (3), 523-536.
- Gudmundsson, O. and M. Sambridge (1998), A regionalized upper mantle (RUM) seismic model. *J. of Geophys. Res.*, No. B4, 7121-7136, 1998.
- Jackson, D.D. (1996) Hypothesis testing and earthquake prediction. *Proceedings of the National Academy of Sciences of the United States of America*, 93, 3772-3775.
- Papadimitriou, E.E.; Evison, F.F.; Rhoades, D.A.; Karakostas, V.G.; Console, R.; Murru, M.R. (2006) Long-term seismogenesis in Greece : comparison of the evolving stress field and precursory scale increase approaches. *Journal of geophysical research. Solid earth*, 111: B05318, doi:10.1029/2005JB003805.
- Rhoades, D.A. (2007) Application of the EEPAS model to forecasting earthquakes of moderate magnitude in southern California. *Seismological Research Letters* 78(1), 110-115
- Rhoades, D.A. and Evison, F.F. (1989). Time-variable factors in earthquake hazard. *Tectonophysics*, 167, 201, 210.
- Rhoades, D.A. and Evison, F.F. (2004). Long-range earthquake forecasting with every earthquake a precursor according to scale. *Pure Appl. Geophys.* 161(1), 47-71
- Rhoades, D.A.; Evison, F.F. (2005) Test of the EEPAS forecasting model on the Japan earthquake catalogue. *Pure and applied geophysics*, 162(6/7): 1271-1290
- Rhoades, D.A.; Evison, F.F. (2006) The EEPAS forecasting model and the probability of moderate-to-large earthquakes in central Japan. *Tectonophysics*, 417(1/2): 119-130
- Schorlemmer, D.; Gerstenberger, M.C. (2007) RELM Testing Center, *Seismological Research Letters*, 78(1), 1-16.
- Schorlemmer, D.; Gerstenberger, M.C.; Wiemer, S.; Jackson, D.D.; Rhoades, D.A. (2007) Earthquake likelihood model testing. *Seismological Research Letters* 78(1), 17-29.
- Shimazaki, K. (1976). Intra-plate seismicity and inter-plate earthquakes: historical activity in Southwest Japan. *Tectonophysics* 33, p. 33.
- Somerville, P.; Fisher, J.; Rhoades, D.; Leonard, M. (2006). Preliminary Test of the EEPAS Long Term Earthquake Forecast Model in Australia. *Proceedings of the 2006 Annual Meeting of the Australian Earthquake Engineering Society.*

## APPENDICES

### APPENDIX 1 TECHNICAL DESCRIPTION OF SUP MODEL

The rate density of the SUP model is defined for any time  $t$ , magnitude  $m$  and location  $(x,y)$  in a region of surveillance  $R$  by

$$\lambda_{\text{SUP}}(t, m, x, y) = \lambda_c \exp[-\beta(m - m_c)] \quad (\text{A1.1})$$

where  $\beta$  and  $\lambda_c$  are constant parameters. Here  $\beta = b \ln(10)$ , where  $b$  is the Gutenberg-Richter  $b$ -value, and the  $\lambda_c$  represents the average rate of occurrence of earthquakes of magnitude  $m_c$  within the region of surveillance.

### APPENDIX 2 TECHNICAL DESCRIPTION OF PPE MODEL

The PPE model (Rhoades and Evison, 2004, 2005) was fashioned from a model proposed by Jackson and Kagan (1999). The rate density  $\lambda_0$  has the form

$$\lambda_0(t, m, x, y) = f_0(t) g_0(m) h_0(t, x, y) \quad (\text{A2.1})$$

where

$$f_0(t) = \frac{1}{t - t_0} \quad , \quad (\text{A2.3})$$

$$g_0(m) = \beta \exp[-\beta(m - m_c)] \quad (m \geq m_0) \quad (\text{A2.3})$$

and  $h_0(t, x, y)$  is the sum, over all earthquakes with  $m \geq m_c$  from time  $t_0$  up to, but not including, time  $t$ , of smoothing kernels of the form

$$h_{0i}(r_i) = a(m_i - m_c) \frac{1}{\pi} \left( \frac{1}{d^2 + r_i^2} \right) + s \quad (\text{A2.4})$$

In equation (A2.3),  $\beta = b \ln(10)$ , where  $b$  is the Gutenberg-Richter  $b$ -value, assumed to be the same throughout the region. In equation (A2.4),  $r_i$  is the distance in km between  $(x,y)$  and the epicentre  $(x_i, y_i)$  of the  $i$ th precursory earthquake; and  $a$ ,  $d$  and  $s$  are constant parameters.

### APPENDIX 3 TECHNICAL DESCRIPTION OF EEPAS MODEL

In the EEPAS model, the rate density  $\lambda(t, m, x, y)$  of earthquake occurrence is defined for any time  $t$ , magnitude  $m$  and location  $(x, y)$ , where  $m$  exceeds a threshold magnitude  $m_c$ , and  $(x, y)$  is a point in a region of surveillance  $R$ . Each earthquake  $(t_i, m_i, x_i, y_i)$  contributes a transient increment  $\lambda_i(t, m, x, y)$  to the future rate density in its vicinity, given by

$$\lambda_i(t, m, x, y) = w_i f_{1i}(t) g_{1i}(m) h_{1i}(x, y) \quad (\text{A3.1})$$

where  $w_i$  is a weighting factor that may depend on other earthquakes in the vicinity, and  $f_{1i}$ ,  $g_{1i}$  and  $h_{1i}$  are densities of the probability distributions for time, magnitude and location, respectively. The magnitude density  $g_{1i}$  is assumed take the form

$$g_{1i}(m) = \frac{1}{\sigma_M \sqrt{2\pi}} \exp \left[ -\frac{1}{2} \left( \frac{m - a_M - b_M m_i}{\sigma_M} \right)^2 \right] \quad (\text{A3.2})$$

where  $a_M$ ,  $b_M$  and  $\sigma_M$  are parameters. The time density  $f_{1i}$  is assumed to take the form

$$f_{1i}(t) = \frac{H(t - t_i)}{(t - t_i) \sigma_T \ln(10) \sqrt{2\pi}} \exp \left[ -\frac{1}{2} \left( \frac{\log(t - t_i) - a_T - b_T m_i}{\sigma_T} \right)^2 \right] \quad (\text{A3.3})$$

where  $H(s) = 1$  if  $s > 0$  and 0 otherwise, and  $a_T$ ,  $b_T$  and  $\sigma_T$  are parameters. The location density  $h_{1i}$  is assumed to take the form

$$h_{1i}(x, y) = \frac{1}{2\pi \sigma_A^2 10^{b_A m_i}} \exp \left[ -\frac{(x - x_i)^2 + (y - y_i)^2}{2\sigma_A^2 10^{b_A m_i}} \right] \quad (\text{A3.4})$$

where  $\sigma_A$  and  $b_A$  are parameters. The total rate density is obtained by summing over all past occurrences, including earthquakes outside  $R$ , which could affect the rate density within  $R$ :

$$\lambda(t, m, x, y) = \mu \lambda_0(t, m, x, y) + \sum_{t_i \geq t_0; m_i \geq m_0} \eta(m_i) \lambda_i(t, m, x, y) \quad (\text{A3.5})$$

where  $\mu$  is a parameter,  $\lambda_0$  is the rate density of the PPE model described in Appendix 2 above,  $t_0$  is the time of the beginning of the catalog and  $\eta$  is a normalizing function.

Rhoades and Evison (2004) proposed two different weighting strategies: a trivial strategy in which all earthquakes are assigned equal weights and a strategy in which aftershocks are down-weighted. The weights in the latter strategy are derived from the rate densities,  $\lambda_0$  and  $\lambda'$ , of a baseline model rate density and a model incorporating aftershocks, respectively:

$$w_i = \frac{v \lambda_0(t_i, m_i, x_i, y_i)}{\lambda'(t_i, m_i, x_i, y_i)}. \quad (\text{A3.6})$$

The aftershock model incorporates epidemic-type aftershock behaviour (Ogata, 1989, 1998; Console and Murru, 2001), albeit with some non-standard features that are designed to admit as aftershocks only earthquakes that are much smaller than the mainshock. The rate density  $\lambda'$  is of the form

$$\lambda'(t, m, x, y) = \nu \lambda_0(t, m, x, y) + \kappa \sum_{t_i \geq t_0} \lambda'_i(t, m, x, y) \quad (\text{A3.7})$$

where  $\lambda_0$  is as above;  $\nu$  and  $\kappa$  are constant parameters; and

$$\lambda'_i(t, m, x, y) = f_{2i}(t) g_{2i}(m) h_{2i}(x, y). \quad (\text{A3.8})$$

Here,  $f_{2i}$ ,  $g_{2i}$  and  $h_{2i}$  are functions for the time, magnitude and location of the aftershocks of the  $i$ th earthquake. The time distribution follows the modified Omori law (e.g. Ogata, 1983); the magnitude distribution has regard to the Gutenberg-Richter law and Båth's law (Båth, 1965; Richter, 1958); and the location distribution is bivariate normal with circular symmetry and has regard to Utsu's areal relation (Utsu, 1961). Thus

$$f_{2i}(t) = H(t - t_i) \frac{p - 1}{(t - t_i + c)^p}, \quad (\text{A3.9})$$

$$g_{2i}(m) = H(m_i - \delta - m) \beta \exp[-\beta(m - m_i)], \quad (\text{A3.10})$$

and

$$h_{2i}(x, y) = \frac{1}{2\pi\sigma_U^2 10^{m_i}} \exp\left[-\frac{(x - x_i)^2 + (y - y_i)^2}{2\sigma_U^2 10^{m_i}}\right], \quad (\text{A3.11})$$

where  $c$ ,  $p$ ,  $\delta$  and  $\sigma_U$  are constant parameters,  $\beta$  is as in equation (A2.3), and the Heaviside function  $H$  as in equation (A3.3).



[www.gns.cri.nz](http://www.gns.cri.nz)

#### Principal Location

1 Fairway Drive  
Avalon  
PO Box 30368  
Lower Hutt  
New Zealand  
T +64-4-570 1444  
F +64-4-570 4600

#### Other Locations

Dunedin Research Centre  
764 Cumberland Street  
Private Bag 1930  
Dunedin  
New Zealand  
T +64-3-477 4050  
F +64-3-477 5232

Wairakei Research Centre  
114 Karetoto Road  
Wairakei  
Private Bag 2000, Taupo  
New Zealand  
T +64-7-374 8211  
F +64-7-374 8199

National Isotope Centre  
30 Gracefield Road  
PO Box 31312  
Lower Hutt  
New Zealand  
T +64-4-570 1444  
F +64-4-570 4657